Health & Safety
Executive

OFFSHORE TECHNOLOGY REPORT- OTO 1999 093

Explosion Resistance of Floating Offshore Installations

Date of Issue: March 2000

Project 3707

Explosion Resistance of Floating Offshore Installations

Prepared by

DERA Rosyth

Summary

The aim of this report is to provide a qualitative assessment in terms of blast loading and failure for typical structural arrangements of floating installations when faced with an idealised gas explosion loading. Four floating installations are examined. These installations will be referred to in this text as Vessel A, B, C and D. The structural response regime of the structures is determined by modal analysis and a dynamic analysis carried out for two load cases. The structural responses of the four structures are then compared on the relative performance.

CONTENTS

1. INTRODUCTION

1.1 BACKGROUND

DERA Rosyth has for a number of years been gathering knowledge, carrying out experiments and developing modelling techniques to assess the loading and failure of steel warship structures when subjected to high explosive (HE) blast loading. This knowledge has, at the request of the Health and Safety Executive (HSE), been applied to modelling the response of floating installations.

The deck structures from four floating installations, which will be referred to as Vessel A, B, C and D, are examined. The purpose of these analyses being to provide an assessment of the ability of deck structure to withstand loading from an idealised hydrocarbon explosion.

Most existing platform topside structures have been designed using static codes of practice. For instance deck structures have been designed to resist static imposed loading from equipment and no allowance has been made for any dynamic pressure caused by explosive loading.

Since the Piper Alpha tragedy and the publication of the Cullen[1] report safety cases are required by the HSE to demonstrate that the offshore platform installation meets stringent safety criteria. This involves assessing the structural response of stiffened deck panels to a given blast loading with the aim of containing or venting the blast to prevent escalation of the consequences of the event.

Floating production, storage and offloading units (FPSOs) have been recently established as attractive alternatives for the exploitation of offshore oil fields, Figures 1 & 2. FPSOs, FPUs and FSU are usually based on barges, converted tankers and purpose built tankers but they still require safety cases.

The report examines the scenario of an explosion in the process modules and superstrucutre of an FPSO class of vessel and the subsequent structural response of the top-deck of the structure. The purpose being to highlight any weakness or characteristic of the structure which could result in failure of the deck and further escalation of the event.

1.2 ASSESSMENT PROCEDURE

As a result of a Joint Industry Project on Blast and Fire Engineering for Topside Structures, Interim Guidance Notes[2] have been issued suggesting techniques for assessing stiffened panel behaviour including the use of transient non-linear finite element techniques.

The assessment procedure used in this report is entirely numerical without any experimental validation. However, DERA Rosyth is a registered ISO 9001 accredited organisation and as such applies quality procedures to its business processes. Numerical analysis forms a large part of DERA Rosyth business and has created a Numerical Modelling Quality Procedure based on NAFEMS and SAFESA quality procedures. As part of this procedure every analysis undergoes rigorous validation. Most numerical work carried out at DERA Rosyth previously has been subjected to experimental validation which is the preferred option. In the absence of experimental information each numerical analysis undergoes a verification procedure to ensure that the numerical model is conforming to the expected behaviour.

The non-linear finite element (FE) code ABAQUS[3-5] has been used to carry out the study. FE models of the four structures were created incorporating geometric and material non-linearity where appropriate and a series of analyses carried out.

Contents

In the first instance, in order to determine the response regimes of the structures a modal analysis was carried out. The extent of damage that can be caused by a blast load greatly depends on the length of time the load acts for, compared to the natural period of the structure. If the loading is impulsive much higher peak loads can be tolerated than if the load were applied over a longer period of time since the structure has insufficient time to respond. If the loading is 'quasi-static', the load duration is much longer than the natural period of the structure and so the full effect of the load is felt. If the period of the loading is in the transition region between these two regimes, *i.e.* close to the period of the structure then the loading is termed 'dynamic'.

References 6 & 7 give a more detailed account but the loading regimes can be summarised by the equations below.

$$0.4 > \omega t_d \quad \left[\propto \frac{t_d \ (short)}{T \ (long)} \right] \quad \text{(Impulsive)}$$

$$40 < \omega t_d \quad \left[\propto \frac{t_d \ (long)}{T \ (short)} \right] \quad \text{(Quasi - static)}$$

$$0.4 < \omega t_d < 40 \quad \left[\frac{t_d}{T} \approx 1 \right] \quad \text{(Dynamic)}$$

where ω is the natural circular frequency of vibration of the structure
t_d is the duration of idealised triangular blast load
T is the natural period of vibration of structure.

This determines which type of analysis is required to assess the response of the structure to dynamic loading. If the response regime lies within either the impulsive or quasi-static regime evaluation of the limits of response can be carried out by considering the energy of the system. If the response regime is dynamic then the structural response behaviour is entirely dependent on the form of the pressure-time history that the structure is subjected to and a dynamic analysis is required. Reference 8 highlights this behaviour and shows the difference in response of a panel due to slightly different pressure-time histories.

The behaviour of the structure is then assessed under two dynamic idealised load cases shown in Figure 3. Load Case 1 refers to an idealised triangular pressure loading with a peak pressure of 0.2MPa, 100ms rise time and 150ms decay. Load Case 2 refers to an idealised triangular pressure loading with a peak pressure of 0.4MPa, 100ms rise time and 150ms decay. These overpressures were not chosen as being typical of the anticipated blast overpressures, but were selected as being in the range of overpressures which would cause structural failure.

From these loadings t_d is 250ms, therefore if the natural frequency of the structure is between 0.25Hz and 25Hz then the structural response is dynamic and a full non-linear structural analysis is required.

1.3 AREAS OF UNCERTAINTY

The main areas of uncertainty associated with these analyses are the effects of equipment mass loading on the structure, the application of the hydrocarbon explosion pressure-time history and the effects of in-plane loading.

The total mass of the structure, mass and location of equipment is known for most of the scenarios, but the details of the connections to the deck are not. It is assumed that the equipment support points are located over the transverse and longitudinal bulkheads so that the effect of mass on the individual deck plate response is minimal. If there is significant mass supported on the transverse frames between bulkheads this is going to decrease the deck natural frequency. However, the effect of this frequency shift will be insignificant as the deck fundamental frequency will have to lower to less than 0.25Hz before any large difference in response behaviour is seen.

The idealised triangular blast loadings are a significant assumption and are extreme load cases as specified the HSE. The effects of congested pipework and process spaces will not be consistent from platform to platform and the load cases are worst case events. It is also assumed that the hydrocarbon explosion is effective across the whole of the deck. This is also a significant assumption for the structures, due to the presence of blast walls and other fixed structures.

In-plane deck loading has not been considered, as not all the information was made available for all the structures. It was deemed necessary to compare the structures on a similar basis so the analyses were carried with no in-plane deck loading. The effect of in-plane tensile loading (hogging) would be to increase the strength of the deck plates, and compressive loading (sagging) to decrease the strength of the deck plates.

Contents

2. VESSEL A

2.1 STRUCTURAL DESCRIPTION

Vessel A is a floating production unit (FPU) which was previously a semi-submersible, self-propelled offshore accommodation vessel weighing approximately 18,000 tonnes and has been converted for oil and gas production.

Reference 9 details the structural drawings supplied by the HSE. Deck 2 is the focus for this analysis and is 82.5m in length and with a width of 64.5m. The supporting structure for the two decks connected to the semi-submerged buoyancy hulls is quite complex but is not the subject of study.

Deck 2 is exposed to a considerable amount of mass loading as it houses all the main machinery and process equipment. For the purposes of the initial analysis, this mass loading is ignored as it is assumed that the mass is distributed over the main supporting structure of the Deck and so has little contribution to the overall deck response.

Insufficient structural information was provided to show how the equipment was attached to Deck 2.

Figure 4 details the supporting longitudinal and transverse bulkhead positions. Vessel A has thirty-three evenly spaced transverse frames starting from Frame -2 at the aft point to Frame 31. There are 6 main transverse bulkheads running the width of the compartment at Frames -2,1,10,19,28 and 31. All have a thickness of 15mm and are manufactured from Lloyd's Grade B steel. There are smaller transverse bulkheads at Frames 23 and 27 localised around the top deck penetration, again Grade B steel with thickness of 7mm and 8mm respectively.

There are 6 longitudinal bulkheads, which are 12mm thick manufactured from Grade B steel. There are also two longitudinal corrugated bulkheads located 6m from the port and starboard edges.

The deck is further stiffened by longitudinal and transverse stiffening, Figure 5. The longitudinal stiffeners are 140x7 bulb flats[10] with a spacing of 0.75m. The transverse stiffeners are T-stiffeners sized from 550x11.5W/150x20T to 250x10W/120x12T.

2.2 FINITE ELEMENT DISCRETISATION

The objective of this analysis is to assess the effects of a hydrocarbon explosion in the process deck of Vessel A. Of primary concern is the performance of Deck 2 under blast loading.

Vessel A has a complex deck structure. The total structure comprising approximately 30 separate panels. It would be normal practice to investigate the performance of the thirty panels separately. However, what boundary conditions would be imposed at the deck panel edge connections?

Without access to modal test data and modal updating software it is virtually impossible to model the behaviour of these deck panels individually. In order to overcome this problem, the whole top deck of Vessel A is modelled. Fully fixed boundary conditions are imposed at the base of the supporting bulkheads. This allows the deck panels to behave realistically without additional modelling assumptions.

The finite element model was created using PATRAN v8. The model contains a total of 20,790 elements comprising of 9488 shell elements and 11302 beam elements. Table 1 below gives a

Contents

breakdown of the finite element model.

Table 1
Vessel A - Finite element model breakdown

Element set	Number of elements	Element type	Description
DCK_8MM	1716	S4R5	Top deck panel, 8mm, Grade B steel
DCK_95MM	1344	S4R5	Top deck panel, 9.5mm, Grade B steel
DCK_15MM	2376	S4R5	Top deck panel, 15mm, Grade B steel
TRAN15MM	1906	S4R5	Transverse bulkheads, 15mm, Grade B steel
LONG15MM	1586	S4R5	Longitudinal bulkheads, 15mm, Grade B
CORG_5MM	216	S4R5	Corrugated bulkheads, 5mm, Grade B
BHD23_7	128	S4R5	Transverse bulkhead at Fr 23, 7mm, Grade B steel
BHD27_8	64	S4R5	Transverse bulkhead at Fr 27, 8mm, Grade B steel
CORR_7MM	72	S4R5	Corrugated bulkhead margin plate, 7mm, Grade B
LIP_EDGE	80	S4R5	Transverse plate at Frame -2, 11.5mm, Grade B
J04140X7	4988	B31	Longitudinal deck stiffeners - 140x7 BP
J06140x7	1660	B31	Vertical transverse bulkhead stiffeners - 140x7 BP
J028140x7	60	B31	Vertical transverse bulkhead stiffeners - 140x7 BP
J07200x9	168	B31	Vertical transverse bulkhead stiffeners - 200x9 BP
J16200X9	78	B31	Vertical transverse bulkhead stiffeners - 200X9 BP
J26200X9	129	B31	Vertical transverse bulkhead stiffeners - 200X9 BP
ANGLEBAR	1188	B31	Horz. Longitudinal bulkhead stiffeners - 100x65x8A
TBAR_J10	240	B31	Long. Bulkhead stiffeners - 250x10W/120x15T
TBAR_J11	448	B31	Long. Bulkhead stiffeners - 250x10W/120x15T
J13_BOX	104	B31	Box bulkhead pillar - 100x100x10
TBAR_J17	846	B31	Trans. deck stiffeners - 550x11.5W/150x20T
TBAR_J18	378	B31	Trans. deck stiffeners - 550x11.5W/250x12T
TBAR_J19	1024	B31	Trans. deck stiffeners - 350x10W/120x12T

Lloyd's Grade B material is used throughout the structure. A non-linear material model was constructed for Lloyd's Grade B. Table 2 below details the material properties used.

Table 2
Lloyd's Grade B material properties

	Grade B
Density (kg/m^3)	7850
Young's Modulus (Pa)	2.05×10^{11}
Poissons Ratio	0.3
Yield Stress (MPa)	235
Ultimate Strength (MPa)	400
Elongation (%)	24

2.3 MODAL ANALYSIS RESULTS

The objective of the modal analysis is to determine the response regime that the structure lies in. Finding the response regime of the structure, as described above, is crucial in the assessment of the structure as it determines the amount of simplification that can be used in the analysis.

The 'egg box' structure of Vessel A, Figure 4, means that the structure has a significant amount of eigenmodes. The modes of interest are the fundamental modes of the individual deck plates

Contents

bounded by the supporting bulkheads.

The first thirty eigenmodes of the structure were calculated and were found to range from 4.9Hz to 14Hz. Most of these calculated mode shapes were fundamental and 2nd order plate modes, the plates being bounded by the supporting structure.

Examples of the fundamental plate modes are shown in Figure 6, Figure 7, Figure 8 and Figure 9. The modal frequencies associated with these mode shapes are 4.9Hz, 7.1Hz, 8.8Hz and 10.0Hz respectively.

It is clear from this that the structure lies within the dynamic response regime and so a full non-linear dynamic finite element calculation is warranted.

2.4 DYNAMIC ANALYSIS RESULTS

Figure 3 details Load Case 1 which is an idealised triangular pressure load with a maximum pressure of 0.2MPa (2bar), with a rise time of 100ms and decay of 150ms. This loading was applied across the whole of the top deck as explained in the scenario definition above.

This analysis could not be completed due to convergence problems in the analysis. Further investigation of the model response shows that the analysis failed to complete because the aft starboard deck plate collapsed shortly after peak load had been attained. Figures 10 and 11 show this unstable behaviour. Figure 12 shows the vertical displacement of the centre of this deck plate. This figure clearly shows the unrestrained displacement of this deck.

The cause of this lack of convergence and instability is probably due to a combination of reasons. The first reason being that the deck has been excessively loaded in this area and the deck has failed. The second reason for instability could be due to inadequate meshing of this particular part of the model. The mesh discretisation may be insufficient to capture, properly, the deformation of the structure. However, it is the authors' opinion that excessive loading is more likely as the mesh discretisation of the plate is sufficient to capture the overall plate behaviour.

On this basis, considering this area of failure is located over hydrocarbon containing equipment between Fr 1 and Fr 10. This is an obvious area of concern as catastrophic collapse of this particular deck area could lead to escalation.

Figure 13 shows the plastic strain distribution across the top deck. There are no real areas of concern other than in the area described above although Figure 13 does show areas of high strain around the corners of the blast walls.

There was little point in carrying out a dynamic analysis with Load Case 2, but it was decided to calculate the load at which instability occurred in that region of the deck. A series of analyses were carried out using the idealised triangular load with maximum pressures of 0.1MPa, 0.125MPa and 0.15MPa. Figure 14 shows the response of the centre of the panel. This figure clearly shows that the dynamic load bearing capacity of this part of the structure is between 0.125MPa and 0.15MPa. This, however, does not mean to say that other parts of the structure will not survive the original load cases.

The original loading scenario specified that a full pressure loading be applied to all parts of the top deck. A more realistic option is for selected parts of the deck to be loaded. However, this can only be defined after a full risk assessment to determine the likely loaded areas and this has not been carried out as part of this study.

Contents

3. VESSEL B

3.1 STRUCTURAL DESCRIPTION

Vessel B is a purpose built FPSO. The design is characterised by port and starboard cargo tanks of an unsymmetric design.

For the purposes of this analysis, the mid-section tank is modelled. Reference 11 details the structural drawings supplied by the HSE. The tank top is modelled from Fr26 - Fr 31, a length of 25m and 38m wide. The tank top thickness is 19mm made from DNV Grade NV36. Frame spacing is 5m. Frames are approximately 17mm thick. The side shell has a thickness of 18mm and is also made from DNV Grade NV36 steel.

The production deck of Vessel B is supported by pedestals over the main deck boundaries. No structural drawings were received for the production deck pedestals but it is assumed that the weight of the production deck will be borne by the watertight boundaries and so will not significantly affect the deck response. Figure 15 shows an end elevation of the vessel with the pedestals over the watertight boundaries.

Longitudinal stiffeners, 380x18W/250x20T, approximately 1.0m apart support the tank top deck. The tank is also supported by a centreline longitudinal bulkhead and girders situated at ±6m and ±10m from the centre.

3.2 FINITE ELEMENT DISCRETISATION

The objective of this analysis is to assess the effects of a hydrocarbon explosion in the production deck of Vessel B and determine whether this deck could be breached by an explosion that would result in further escalation of the event.

Symmetry of the structure is used, thus allowing a 'half model' to be created, saving computing time. Symmetric boundary conditions are applied to the Fore and Aft boundaries of the model. Figure 16 shows an isometric view of the finite element mesh. Forward direction is defined by the positive x-axis, port by the positive y-axis and vertical by the positive z-axis

Figure 17 clearly shows the port & starboard cargo tanks. A longitudinal bulkhead splits the tanks. Note also that the port side tank has more supporting structure than the starboard and so the deck structure above this tank will be stiffer.

Figure 17 also shows the longitudinal stiffening, the main longitudinal girders represented by shells and supporting stiffening represented as beams.

The full height of the side shell structure is not modelled because the deck response is of primary interest. Fully fixed boundary conditions are used at the base of the model. The finite element model was created using PATRAN v8. The model contains a total of 7321 elements comprising 5846 shell and 1475 beam elements. Table 3 gives a breakdown of the finite element model.

The structure was constructed with DNV Grade NV36. This steel is equivalent to ASTM A131M-94 Grade DH36. Table 4 details the material properties used.

Contents

Table 3
Vessel B - Finite element model breakdown

Element set	Number of elements	Element type	Description
DECK	1900	S4R5	Tank top deck, 19mm, DNV-NV36
FR27	517	S4R5	Frame 27, 17mm, DNV-NV36
FR28	517	S4R5	Frame 28, 17mm, DNV-NV36
FR26_TNK	912	S4R5	Tank Bulkhead, 17mm, DNV-NV36
SSHELL	600	S4R5	Side shell, 18mm, DNV-NV36
SECT_16	1000	S4R5	Longitudinal girder, 16mm, DNV-NV36
SECT_20	300	S4R5	Centre longitudinal bulkhead, 20mm, DNV-NV36
SECT_25	100	S4R5	L shaped girder, 16mm, DNV-NV36
SHELL_ST	625	B31	Long. side shell stiffeners, 330x16W/200x20T
DECK_ST	750	B31	Long. Deck stiffeners, 380x18W/200x20T
LONG_ST	100	B31	Long. Girder stiffeners, 200x16

Table 4
Material properties DNV Grade NV36

	Grade DH36
Density (kg/m^3)	7850
Young's Modulus (Pa)	2.05×10^{11}
Poissons Ratio	0.3
Yield Stress (MPa)	360
Ultimate Strength (MPa)	490
Elongation (%)	22

3.3 MODAL ANALYSIS RESULTS

The objective of the modal analysis is to determine the response regime in which the structure lies.

The first hundred eigenmodes were calculated. Again this is a modally rich structure with the first hundred eigenmodes having frequencies up to 38.7Hz. Figure 18 & Figure 19 show the global deck response mode for the Starboard and Port tanks. These frequencies are 27.5Hz and 34.1Hz respectively. The Port tank top has the higher frequency as anticipated.

These frequencies just fall into the range of quasi-static behaviour, the cut-off being 25Hz. However, there are many other modes under 25Hz. Figure 20 and Figure 21 show examples of two modes which have frequencies less than 25Hz and which would significantly affect the deck response.

Since a significant amount of the deck response behaviour lies in the dynamic regime it was decided that a full dynamic analysis was required.

3.4 DYNAMIC ANALYSIS RESULTS

Figure 3 details Load Case 1 which is an idealised triangular pressure load with a maximum pressure of 0.2MPa (2bar), with a rise time of 100ms and decay of 150ms. This loading was applied across the whole of the tank top deck.

Contents

Figure 22 shows the displacement-time history of the centre of the Port and Starboard tanks. The starboard tank is clearly less stiff than the port tank. Peak displacement occurs 130ms into the analysis, 30ms after the peak loading has been applied. Figure 23 shows a contour plot of vertical displacement at this time. This plot shows the difference in displacement between the two tanks.

The aspect ratio of the tank top means that the main stress direction will be Fore/Aft. Figure 24 shows a stress contour plot of the cargo tanks at peak displacement. This figure shows stresses just above yield at the watertight bulkhead connection. Figure 25, a strain contour plot, confirms that yielding has occurred.

Figure 26 shows the increased peak displacement of the tank top under this load and also the increased residual displacement. Figure 27 shows a displacement contour plot at the time of peak displacement, 155ms.

Figure 28 shows significantly higher stresses than for load case1 with a large portion of the main deck yielding. Figure 29, a fore/aft strain contour plot, shows yielding at the watertight bulkhead of the tank with strains in excess of 5%.

If these levels of strain occurred at a welded connection they would probably be sufficient to induce plate rupture. However, this depends on whether the main deck plate is continuous across the cargo tank watertight bulkheads.

Contents

4. VESSEL C

4.1 STRUCTURAL DESCRIPTION

Vessel C is a tanker refitted as an FPSO. The vessel underwent major rebuilding with the bow and stern removed, upgraded and joined to a new mid section.

For the purposes of this analysis, the mid-section tank is modelled. Reference 12 details the structural drawings supplied by the HSE. This cargo tank runs from Frame 69 to Frame 74, a length of 24m, and is 34m wide. The cargo tank top/main deck is 30mm thick and made from DNV Grade NVD32. Frame spacing is 4.8m. Frames are approximately 12mm thick. Figure 30 shows a typical frame detail which shows that there is considerable bracing to the main deck.

Process equipment is supported on a mezzanine deck and it is assumed the supports for this occur at the main watertight boundaries of the cargo tanks and so mass loading is not a concern.

Longitudinal stiffening is provided by six girders spaced at 5m intervals. Additional longitudinal stiffening is provided by T stiffeners of dimensions 375x20W/200x30T spaced at 1m intervals.

4.2 FINITE ELEMENT DISCRETISATION

Symmetry of the structure is used, allowing a 'quarter model' to be created, which reduces computing time considerably. Symmetric boundary conditions are applied to the Fore and Aft boundaries of the model and along the longitudinal centreline of the cargo tank. Figure 31 shows an isometric view of finite element mesh. Forward direction is defined by the positive x-axis, port by the positive y-axis and vertical by the positive z-axis

Figure 31 shows the inner and outer hull of the cargo tank and the longitudinal girders. The angled nature of the transverse frame is also apparent.

The full height of the side shell structure is not modelled because the deck response is of primary interest. Fully fixed boundary conditions are used at the base of the model. The finite element model was created using PATRAN v8. The model contains a total of 6237 elements comprising 4020 shell and 2217 beam elements. Table 5 gives a breakdown of the finite element model.

The structure was constructed with four different grades of steel, DNV Grade NVA-NS, Grade NVA-32, Grade NVB-NS and Grade NVD-32. These steels are equivalent to ASTM A131M-94 Grade A, Grade AH32, Grade B and Grade DH32. Table 6 details the material properties used.

4.3 MODAL ANALYSIS RESULTS

A modal analysis was conducted and the first fifty eigenmodes calculated. Figure 32 and Figure 33 show the first and second main deck modes of Vessel C at 15.0Hz and 25.1Hz respectively.

Figure 33 clearly shows that the deck behaviour will be governed by two main responses, that of the largely unsupported centre deck structure and that of an area from the outer hull to the outermost longitudinal girder on the starboard side (starboard wing tank).

Contents

Table 5
Vessel C - Finite element model breakdown

Element set	Number of elements	Element type	Description
DECK	850	S4R5	Main deck, 30mm, Grade DH32
FR69_BHD	1192	S4R5	Cargo tank WTB, 20mm,Grade B
FR70	264	S4R5	Transverse frame 70, 12mm, Grade B
FR71	264	S4R5	Transverse frame 71, 12mm, Grade B
LONG_15	100	S4R5	Centreline girder, 15mm, Grade DH32
LONG_30	275	S4R5	Long. girder, 30mm, Grade DH32
LONG_25	300	S4R5	Red. thickness girder table, 25mm, Grade DH32
ANGLE_20	150	S4R5	Inner hull angled section, 20mm, Grade A
ANGLE_22	100	S4R5	Inner hull angled section, 22mm, Grade AH32
SECT_17	100	S4R5	Inner hull plate, 17mm, Grade A
SECT_18	50	S4R5	Inner hull plate, 18mm, Grade A
SECT_19	150	S4R5	Inner hull plate, 19mm, Grade A
SECT_20	150	S4R5	Inner hull plate, 20mm, Grade A
SECT_21B	150	S4R5	Inner hull plate, 21mm, Grade AH32
STRINGER	200	S4R5	Plate between Inner & Outer hull, 12mm, Grade B
SS_25	150	S4R5	Outer hull plate, 25mm, Grade DH32
SS_21	150	S4R5	Outer hull plate, 21mm, Grade DH32
SS_19	150	S4R5	Outer hull plate, 19mm, Grade DH32
SS_18	400	S4R5	Outer hull plate, 18mm, Grade DH32
ANGLE_ST	100	B31	Long., 350x14W/200x20T, Grade A
DECK_BR1	25	B31	Long., Rect. deck stiffening, 350x25, Grade DH32
DECK_BR2	50	B31	Long., Rect. deck stiffening, 350x25, Grade DH32
DECK_ST	350	B31	Long., 375x20W/200x30T, Grade DH32
STRING_ST	150	B31	Long., Rect. 200x15, Grade A
TRANS_ST	48	B31	Trans., Rect., 200x15,, Grade A
HOLE_ST	44	B31	Stiff. around frame penetration, 150x15, Grade A
SS-BOT-I	125	B31	Vert. Stiff. inner hull, 500x14W/180x20T, Grade ?
SS-BOT-01	100	B31	Vert. Stiff. outer hull, 500x14W/200x20T, Grade ?
SS-BOT-02	25	B31	Vert. stiff. outer hull, 500x14W/200x20T, Grade AH32
SS-MID-I	125	B31	Vert. Stiff. inner hull, 500x11W/165x15T, Grade A
SS-MID-O	125	B31	Vert. stiff. outer hull, 500x11W/180x15T, Grade B
SS-TOP-01	50	B31	Vert. stiff. outer hull, 350x14W/200x20T, Grade DH32
SS-TOP-02	50	B31	Vert. stiff. outer hull, 350x14W/200x20T, Grade AH32

Table 6
Material properties

	Grade A	Grade B	Grade AH32	Grade DH32
Density (kg/m^3)	7850	7850	7850	7850
Young's Modulus (Pa)	2.05×10^{11}	2.05×10^{11}	2.05×10^{11}	2.05×10^{11}
Poissons Ratio	0.3	0.3	0.3	0.3
Yield Stress (MPa)	235	235	315	315
Ultimate Strength (MPa)	400	400	470	490
Elongation (%)	24	24	22	22

Contents

The 15Hz main deck response clearly lies in the dynamic regime well below the 25Hz cut-off, but the secondary deck response at 25.1Hz is only just considered dynamic. Detailed examination of the modal analysis results show that the contribution to the response from this second mode is almost the same as the first mode, *ie* 15.0Hz mode contributes 18.5%, and 25.1Hz mode contributes 14.4%. Also, the 25.1Hz mode, influences not only the wing tank displacement but the main cargo tank centre displacement as well.

4.4 DYNAMIC ANALYSIS RESULTS

Figure 3 details Load Case 1 which is an idealised triangular pressure load with a maximum pressure of 0.2MPa (2bar), with a rise time of 100ms and decay of 150ms. This loading was applied across the whole of the tank top deck.

Figure 34 shows the displacement-time history of the centre of the cargo tank and the centre of the starboard wing tank. The wing tank is clearly less stiff than the main cargo tank. Figure 35 shows a contour plot of vertical displacement at this time. This plot clearly shows the difference in displacement between the two tanks.

Initially this seems incorrect as the mode shape with the lowest natural frequency should give the dominant behaviour. However, as described above, the 15Hz mode and the 25Hz mode have similar contributions to the overall response behaviour. The question then arises, 'How can the 25Hz mode be excited if it is not in the dynamic response regime?'.

This can be explained by the influence of geometric and material non-linearity. These cause the stucture to have an overall reduced stiffness, which in turn reduces the modal frequencies to such an extent that 15Hz and 25Hz mode reduce to 13.7Hz and 14.2Hz, both well within the dynamic response regime.

Figure 36 and Figure 37 show stress contour plots of the cargo tanks at peak displacement in the Fore/Aft and Port/Stbd directions. These figures show high stresses, just above yield, at the watertight bulkhead connection and at the outermost longitudinal girder.

Load case 2, 0.4MPa peak loading induces a much larger structural response. Figure 38 clearly shows the increased peak displacement of the tank top under this load and also the increased residual displacement. Figure 39 shows a displacement contour plot at the time of peak displacement, 163ms.

The fore/aft direction stress of load case 2, Figure 40, shows significantly higher stresses than load case 1 with a large portion of the main deck yielding. Stresses in the port/stbd direction have less of a contribution under this loading, Figure 41. This is probably due to the outer hull of being pulled in and so reducing stress at the connection. Figure 42, a fore/aft strain contour plot, shows yielding at the watertight bulkhead of the tank with strains in excess of 5%.

If these levels of strain, occurred at a welded connection they would probably be sufficient to induce plate rupture. However, again, this depends on whether the main deck plate is continuous across the cargo tank watertight bulkheads.

Contents

5. VESSEL D

5.1 STRUCTURAL DESCRIPTION

Vessel D is a Floating Storage Unit (FSU), essentially a moored tanker. Crude oil is pumped to the storage tanker and then exported via shuttle tankers.

For the purposes of this study the midships cargo tank, from Frame 60 - Frame 67, is analysed. The tank is 42m wide and 26.6m in length. The central portion of the deck is horizontal with a 4° slope towards the hull. The deck is constructed from 22mm, Grade DH32 steel.

The deck is strengthened longitudinally by flat plate stiffeners, 330x28, running the length of the deck with a transverse spacing of 880mm. The deck is further stiffened by three longitudinal girders, 2950x16W/600x16T made from Grade DH32 steel. These deep web girders are additionally stiffened by three uniformly spaced horizontal plate stiffeners, 220x14 projected out from the girder web.

Vessel D as with most commercial oil transportation has a double hull/water ballast tank arrangement. Transverse stiffening is provided by detailed hull frames with a spacing of 3.8m. Additional transverse support is provided by stringers.

The main watertight bulkheads for the tanks are situated at Fr 60 and Fr 67. These bulkheads are of variable width and have three transverse supporting girders.

5.2 FINITE ELEMENT DISCRETISATION

Symmetry of the structure is used, allowing a 'quarter model' to be created, which reduces computing time considerably. Symmetric boundary conditions are applied to the Fore and Aft boundaries of the model and along the longitudinal centreline of the cargo tank. Figure 43 shows an isometric view of the finite element mesh. Forward direction is defined by the positive x-axis, port by the positive y-axis and vertical by the positive z-axis.

Figure 44 shows the inner and outer hull of the cargo tank and the longitudinal girders. A straight double hull/water ballast tank strucutre similar to Vessel B is evident.

The full height of the side shell structure is not modelled because the deck response is of primary interest. Fully fixed boundary conditions are used at the base of the model. The finite element model was created using PATRAN v8. The model contains a total of 5492 elements comprising 4126 shell and 1366 beam elements. Table 7 gives a breakdown of the finite element model. The structure was constructed with two different grades of steel. It is assumed these are equivalent to ASTM A131M-94 Grade D and ASTM-131M-94 Grade DH32.

5.3 MODAL ANALYSIS RESULTS

A modal analysis was conducted and the first fifty eigenmodes calculated. Figure 45 and Figure 46 show the first and second main deck modes of Vessel D at 12.8Hz and 24.2Hz respectively. The fundamental and second deck modes of Vessel D lie in the dynamic regime. This clearly indicates that a full non-linear dynamic analysis is warranted. An extreme response can be expected due to the fact that the first two main deck modes are within the dynamic response regime.

Contents

Table 7
Vessel D - Finite element model breakdown

Element set	Number of elements	Element type	Description
BHD_60	793	S4R5	Blkhd at Frame 60, 11mm, Grade D
CL_GRDR	160	S4R5	Centreline girder, 16mm, Grade DH32
DECK	830	S4R5	Deck, 22mm, Grade DH32
FR_60_BHD	155	S4R5	Blkhd at Frame 60, 12mm, Grade D
FR61	374	S4R5	Frame 61, 12mm, Grade D
FR62	374	S4R5	Frame 62, 12mm, Grade D
FR63	374	S4R5	Frame 63, 12mm, Grade D
GIRDER_2	148	S4R5	Long. girder, 16mm, Grade D
GRDR_STF	54	S4R5	Grider stiffener,16mm, Grade D
GRD2_STF	54	S4R5	Girder stiffener, 14mm, Grade D
IN_SHL18	126	S4R5	Inner hull shell, 18mm, Grade DH32
IN_SH16	270	S4R5	Inner hull shell, 16mm, Grade DH32
OUTSHL22	144	S4R5	Outer hull shell, 22mm, Grade DH32
OUTSHL17	270	S4R5	Outer hull shell, 17mm, Grade DH32
BRACKETS	54	B31	Rect plate, 200x12mm, Grade D
DECK_ST	378	B31	Deck stiffeners, 300x12mm, Grade DH32
FRM_TBLS	168	B31	Frame tables, 300x12mm, Grade D
GRD2_BMS	18	B31	Long. girder table, 600x16mm, Grade D
GRDR_BMS	18	B31	Long. girder table, 600x16, Grade D
HORGRD1	38	B31	Horz girders on Fr 60, 630x16mm, Grade D
HORGRD2	76	B31	Horz girders on Fr 60, 2000x12W/250x15T, Grade D
IN_B1	54	B31	Hull stiffeners, 330x22mm, Grade DH
IN_T1	36	B31	Hull stiffeners, 300x11W/100x14T, Grade D
IN_T2	72	B31	Hull stiffeners, 325x11W/120x14T, Grade D
IN_T3	18	B31	Hull stiffeners, 375x11W/120x15T, Grade D
OUT_B1	54	B31	Hull stiffeners, 330x22mm, Grade DH
OUT_T1	36	B31	Hull stiffeners, 300x11W/100x14T, Grade D
OUT_T2	72	B31	Hull stiffeners, 325x11W/120x14T, Grade D
OUT_T3	18	B31	Hull stiffeners, 375x11W/120x15T, Grade D
STRING_1	136	B31	Trans. stiffener, 275x11W/100x12T, Grade D
STRING_2	96	B31	Trans. stiffener, 300x11W/100x14T, Grade D
STRING_3	24	B31	Trans. stiffener, 325x11W/120x15T, Grade D

Table 8
Material properties

	Grade D	Grade DH32
Density (kg/m^3)	7850	7850
Young's Modulus (Pa)	2.05×10^{11}	2.05×10^{11}
Poissons Ratio	0.3	0.3
Yield Stress (MPa)	235	315
Ultimate Strength (MPa)	400	490
Elongation (%)	24	22

Contents

5.4 DYNAMIC ANALYSIS RESULTS

Figure 3 details Load Case 1 which is an idealised triangular pressure load with a maximum pressure of 0.2MPa (2bar), with a rise time of 100ms and decay of 150ms. This loading was applied across the whole of the tank top deck.

Figure 47 shows the displacement-time history of the centre of the cargo tank. A maximum displacement of 1.3m occurs 180ms into the loading. Figure 48 shows a contour plot of vertical displacement at this time.

Again, the aspect ratio of the tank top means that the main stress direction will be in the fore/aft direction for the centre of the cargo tank. Figure 49 and Figure 50 show stress contour plots of the cargo tank at peak displacement in the Fore/Aft and Port/Stbd directions. These figures show high stresses through the whole plate in the Fore/Aft direction and at the inner hull boundary in the Port/Stbd direction. Figure 51 shows the strain in the Fore/Aft direction. The majority of the high plastic strains are seen near the watertight boundary connection with strains between 3-5%. Strains at this level could induce failure of a welded connection.

Load case 2, 0.4MPa peak loading, induces a much larger structural response. Figure 52 clearly shows the increased peak tank top displacement of 3.2m, and an increased residual displacement. Figure 53 shows a displacement contour plot at the time of peak displacement, around 180ms.

The fore/aft direction stress of load case 2, Figure 54, shows lower stresses than load case 1 although there is a larger contribution around the inner hull connection. Figure 55, shows this increase in stress in the Port/Stbd direction.

This can be explained by the fact that the watertight boundary connection has under gone significant yielding and a plastic hinge has formed such that no more load can be supported. Therefore there is a corresponding increase in stress near the inner hull boundary. Figure 56 confirms this by indicating strains between 5-10% at the watertight boundary connection.

The levels of strain occuring at this connection would probably be sufficient to induce plate rupture.

Contents

6. DYNAMIC RESPONSE COMPARISON

6.1 DISPLACEMENT RESPONSE

Figure 57 shows a comparison of the deck responses of the four offshore installations to Load Case 1. The figure includes the Vessel A results for comparison where the maximum pressure was reduced to 0.15MPa.

It is clear from this figure that Vessel B and Vessel C have similar dynamic performance. This is not surprising since they were both purpose built for a similar job (albeit that Vessel C was a refit) and so will have been built to similar standards. The approach to the design is however different.

Vessel B has a system of internal cargo tanks that are separated port and starboard by a centreline bulkhead, and has a set of water ballast tanks on the outside of the tanks. Vessel C has one central tank and a system of deep girders. Also the main deck thickness is different. Vessel B has a deck thickness of 19mm, Vessel C a deck thickness of 30mm.

Vessel D and Vessel A experience considerable displacements, when compared with Vessel B and Vessel C, indicating more dynamically responsive structures. As discussed earlier, the structural response is influenced by the duration of the loading and the natural frequency of the structure. Of the four structures, Vessel A and Vessel D were the only two where the 1st and 2nd order plate modes lay within the dynamic regime.

Figure 58 shows a comparison of the deck responses due to Load Case 2. As expected higher responses are seen, with considerable residual displacements. Once again, Vessel B and Vessel C have similar responses with peak displacements approximately 1.5m but Vessel D has a maximum displacement of approximately 3.2m. The potential consequences of these high displacements are significant, the main consequence is reduction in overall hull girder strength and the possibility of hull girder collapse as a result of the ballast condition and sea state.

6.2 RELATIVE PERFORMANCE

Table 9, below details the relative performance of the four offshore installations.

Table 9
Relative performance of offshore platforms

	Load Case 1	Load Case 2
Vessel A	X	X
Vessel B	✓	✓/X
Vessel C	✓	✓/X
Vessel D	✓	X

✓ - Survive ✓/X - Possible Fail X - Fail

Vessels B, C and D will, given the loading and modelling assumptions, survive Load Case 1, a 0.2MPa, 100ms rise, 150ms decay, idealised triangular loading. Vessel A will in all probability survive at least a 0.125MPa peak pressure loading.

All of the offshore platform production decks considered in this study have a high likelihood of rupture after Load Case 2 which may lead to an escalation of the explosive event. However, the details of the rupture or failure is directly dependent on local details. If there is continuous deck plating across the watertight bulkhead connection, then rupture may not occur. DERA Rosyth has evaluated the performance of conventional welded connections under transverse dynamic loading and concluded that failure is likely in the heat affected zone of a ferritic weld at between 4-5% strain.

Contents

7. CONCLUSIONS & RECOMMENDATIONS

7.1 CONCLUSIONS

The analyses conducted here have shown that the deck responses of the four offshore installations, Vessels A, B, C and D, all lie within the dynamic response regime for the load cases studied.

The assessment of structural response in this regime is complex and requires the complete solution of the equations of motion of the structure because the response depends upon the form of the pressure-time history.

Vessel B and Vessel C both withstood load case 1 (2 bar) with very little permanent displacement. At this load level the Vessel A analysis failed due to either buckling and instability caused by weak supporting structure and the size of deck plate that was subjected to loading or inadequate meshing. It is the author's opinion that the instability is due to excessive loading. Vessel D incurred large plastic deformations at a level which would be considered survivable.

Under load case 2 (4 bar) both Vessel A and Vessel D would have failed completely and Vessel B and Vessel C would possibly fail. Actual determination of failure using the FE code ABAQUS/Standard is subjective but DERA Rosyth's experience of blast loaded bulkheads indicates that failure is likely.

It is not possible to conclude anything about the different construction methods used as no parametric design studies have been conducted. However, the analysis carried out highlights the importance of determining the response regime for a particular design.

Dynamic design methods for offshore structures are in their infancy and do not form the major toolset for the naval architect. Simplistic dynamic analyses using single degree of freedom systems have their place in design but as the analyses above have shown the contribution from 2^{nd} order modes can be significant if they respond dynamically. Modal analysis should form the basis of any safety case that is carried out on an offshore installation deck structure to establish whether the response of the deck needs to be evaluated by a full non-linear dynamic analysis and consequently ensure that the appropriate design process is adopted.

7.2 RECOMMENDATIONS

The complexity of the four structures analysed, and the requirement to do a comparative study precluded detailed analysis of each individual structure in the time-scale of the project. In particular the problems associated with the Vessel A structure need to be investigated in more detail. It is recommended that further and more detailed analyses of Vessel A are carried out.

All of the above analyses, except the Vessel A study, made assumptions regarding the boundary conditions of the watertight tank bulkhead. In reality there will be some flexibility associated with this bulkhead which will influence the response of the main deck structure. It is recommended that the influence of this boundary condition assumption is examined in more detail.

Determination of the response regime was done with reference to Biggs[7], by a very simple method. This could be improved by analysing the pressure-time history in the frequency domain (energy spectral density) and comparing with modal analysis results and thus providing an improved method of determining which modes of the structure will be excited. Using this

Contents

method it is then simple to determine which load cases are important. It is recommended that more realistic pressure-time histories are investigated in terms of energy spectral density to establish the important load cases.

In-plane loading due to sagging and hogging has not been investigated. More detailed information is required before this can properly accounted for. The effect of in-plane tensile loading (hogging) would be to increase the strength of the deck plates, and compressive loading (sagging) to decrease the strength of the deck plates. It is recommended that some studies are carried out to highlight the difference in responses due to this type of loading.

Contents

8. REFERENCES

1. Cullen, Lord, *The Public Inquiry into the Piper Alpha Disaster*. HMSO, UK, 1990
2. Anon. *Interim Guidance Notes for the Design and Protection of Topside Structures against Explosion & Fire*, SCI-P-112. The Steel Construction Institue, UK 1992
3. Anon., *ABAQUS/Standard v5.7 User's Manual Vol I-III*, Hibbitt, Karlsson & Sorenson, 1997
4. Anon., *ABAQUS/Standard v5.7 Theory Manual*, Hibbitt, Karlsson & Sorenson, 1997
5. Anon., *ABAQUS/Standard v5.7 Verification Manual*, Hibbitt, Karlsson & Sorenson, 1997
6. Anon., *Blast and Fire Engineering Project for Topside Strucutres - Blast Response Series* February 1991
7. Biggs, J. M., *Introduction to Strucutral Dynamics* McGraw-Hill, New York 1964
8. Louca L. A., et al. *Non-linear Analysis of Blast Walls and Stiffened Panels Subjected to Hydrocarbon Explosions* J. Construct. Steel Res., Vol37 No 2, pp99-113 , Elsevier Science Ltd, 1996
9. Private Communication - *Vessel A drawings* - Various, HSE, December 1998
10. BS4848:Part5:1980, *'British Standard Specification for Hot rolled structural steel sections - Part 5 Bulb flats'* 1980
11. Private Communication - *Vessel B drawings* - Various, HSE, December 1998
12. Private Communication - *Vessel C drawings* - Various, HSE, December 1998
13. Private Communication - *Vessel D drawings* - Various, HSE, December 1998
14. Misselbrook, N K Unpublished DERA Report DERA/SS/SV/TR971036 Dec 1997.

Contents

9. FIGURES

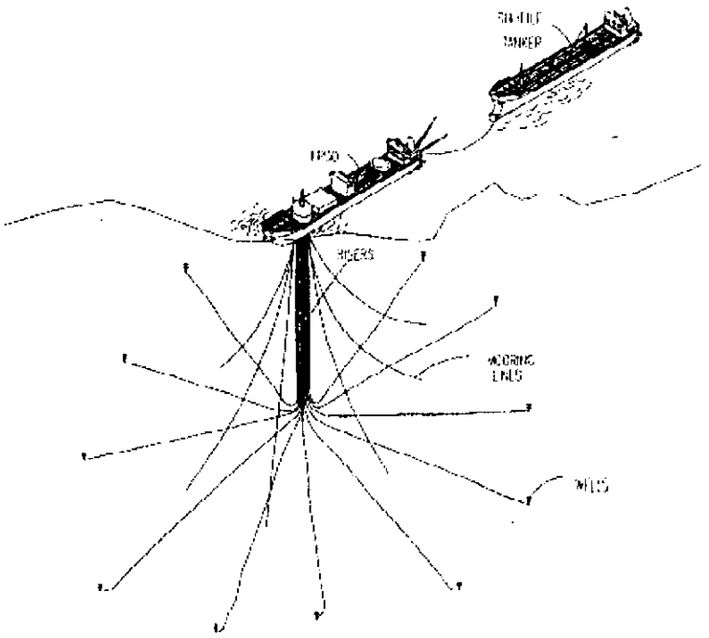

Figure 1
General view of a FPSO unit[8]

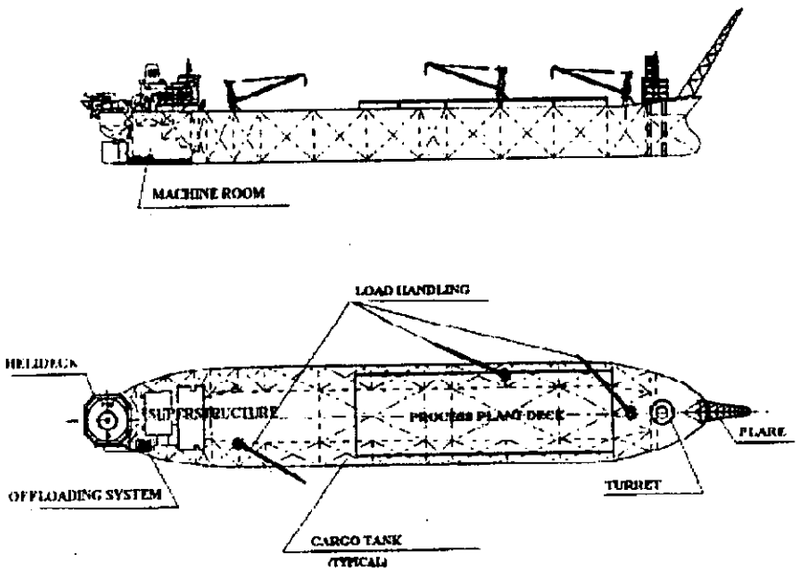

Figure 2
Schematic representation of a FPSO[8]

Contents

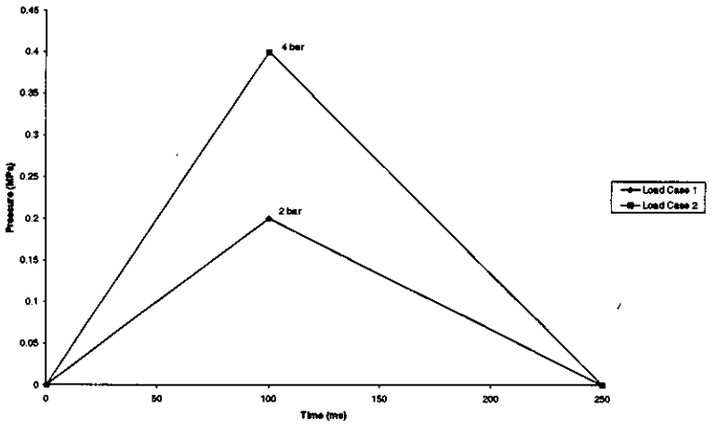

Figure 3
Dynamic load cases

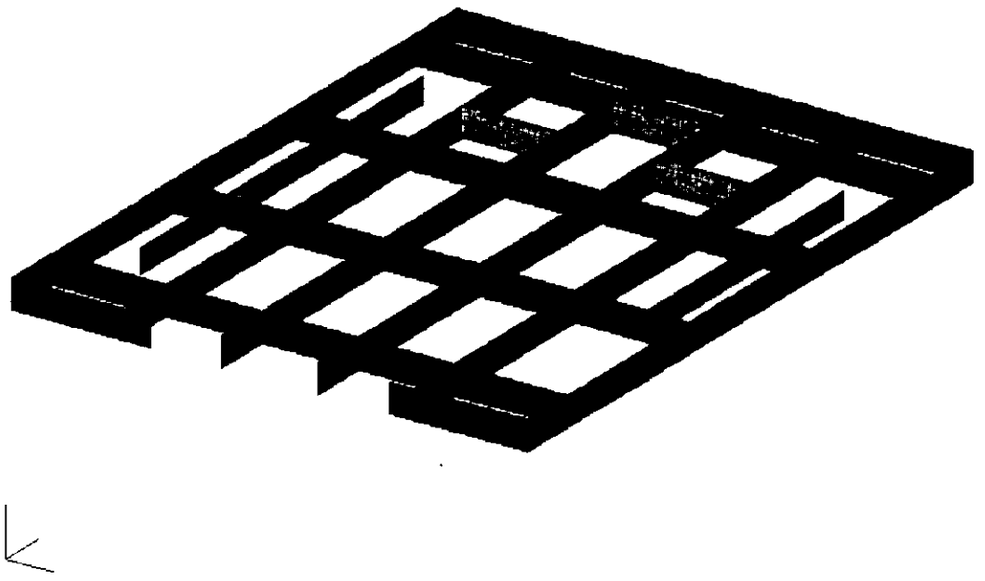

Figure 4
Vessel A - Longitudinal & Transverse bulkhead positions

Contents

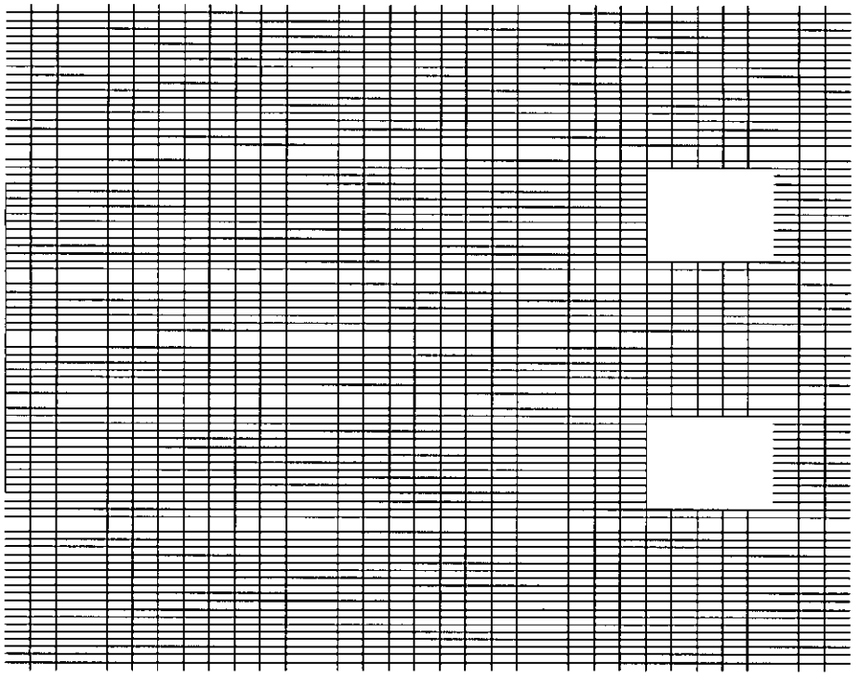

Figure 5
Vessel A - Longitudinal and transverse stiffener layout

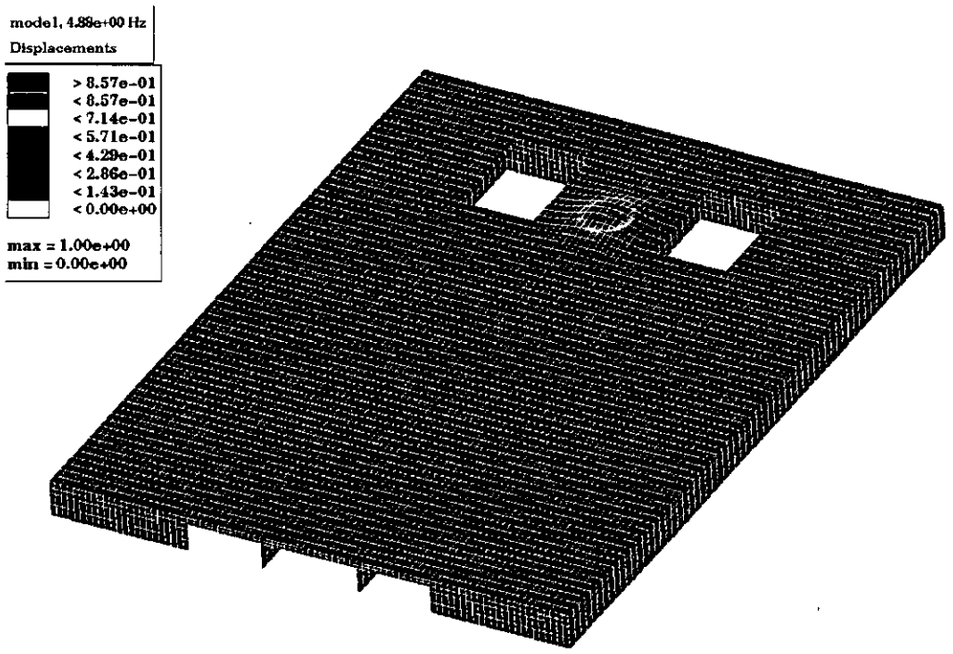

Figure 6
Eigenmode 1 - Deck plate mode - 4.9Hz

Contents

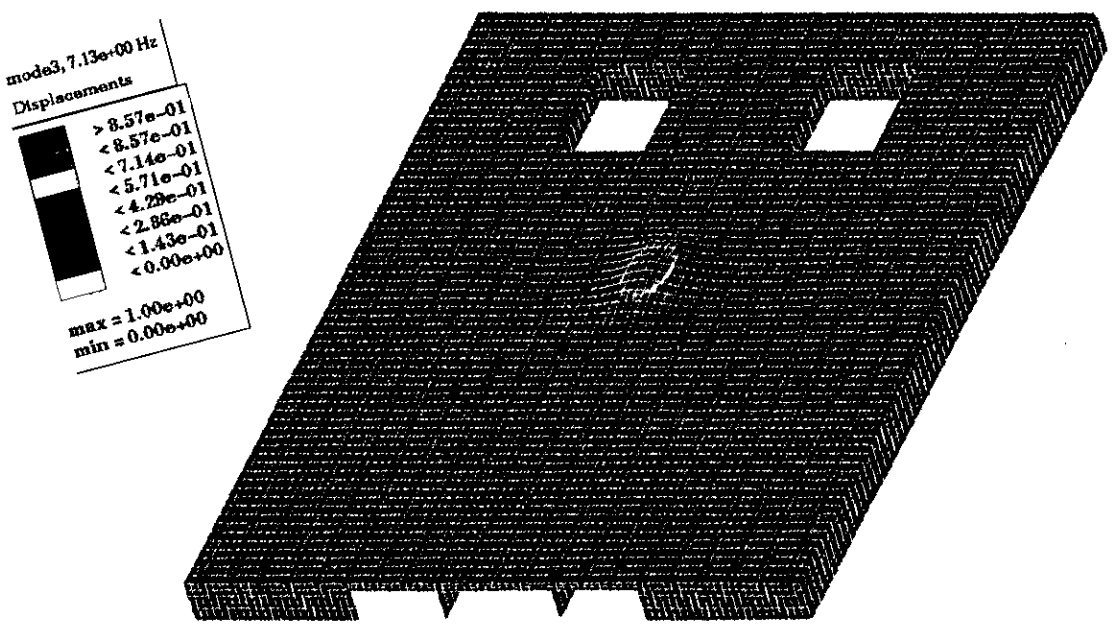

Figure 7
Eigenmode 3 - Deck plate mode - 7.1Hz

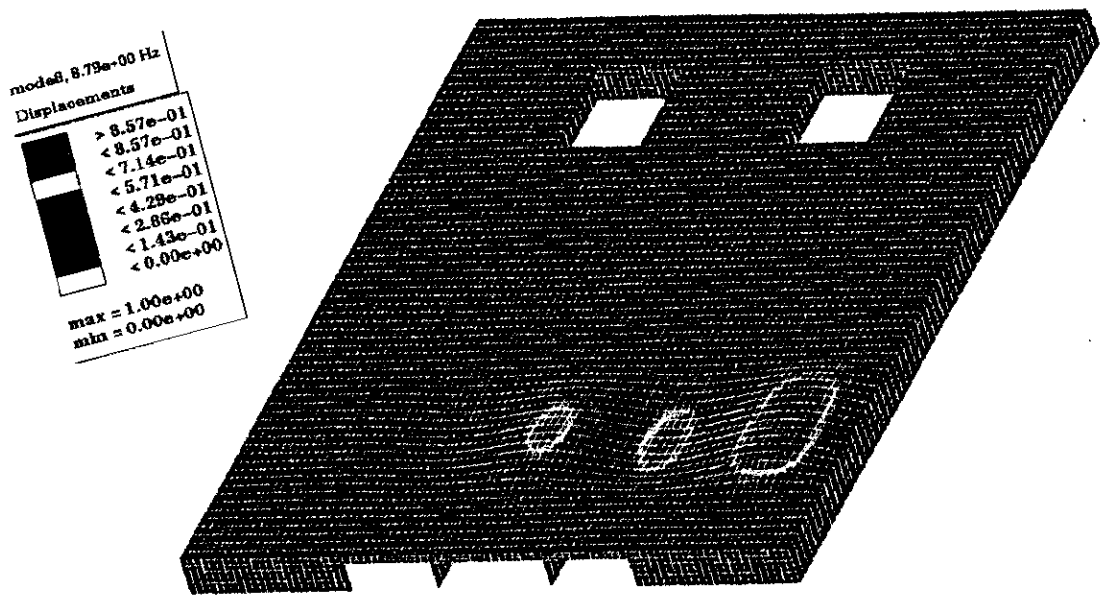

Figure 8
Eigenmode 6 - Deck plate mode - 8.8Hz

Contents

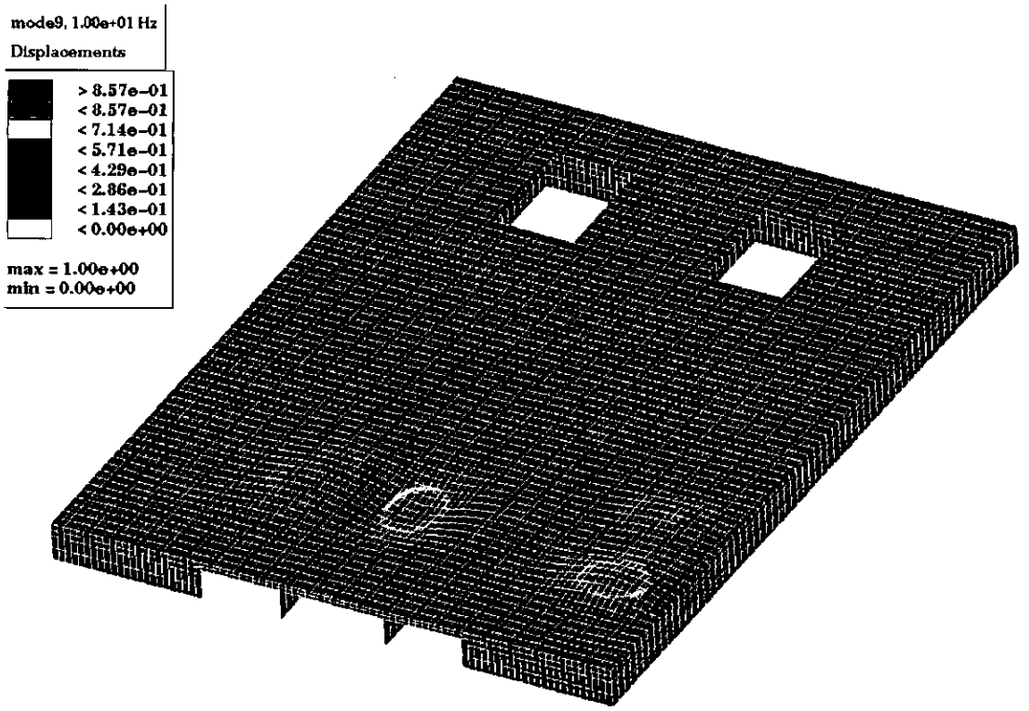

Figure 9
Eigenmode 9 - Deck plate mode - 10.0Hz

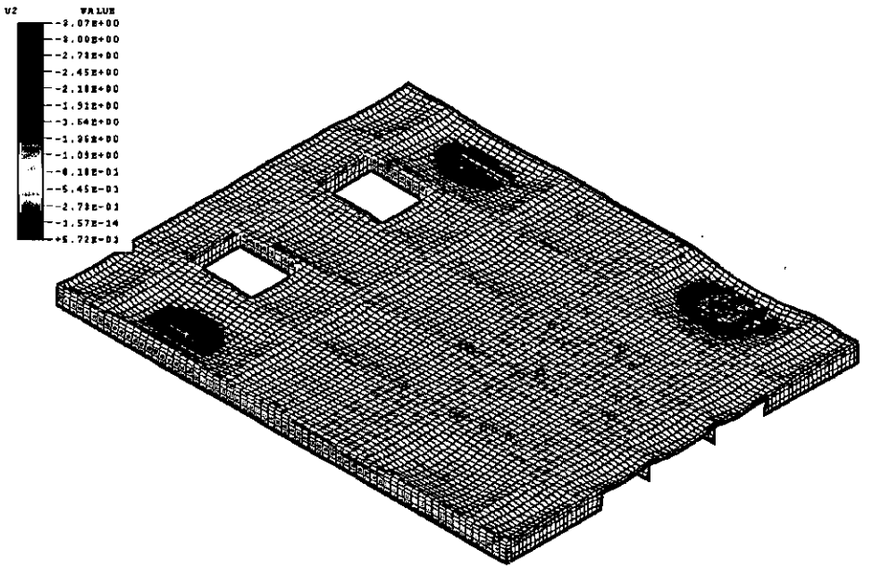

Figure 10
Dynamic Analysis - Load Case 1 Contour plot of Vertical displacement

Contents

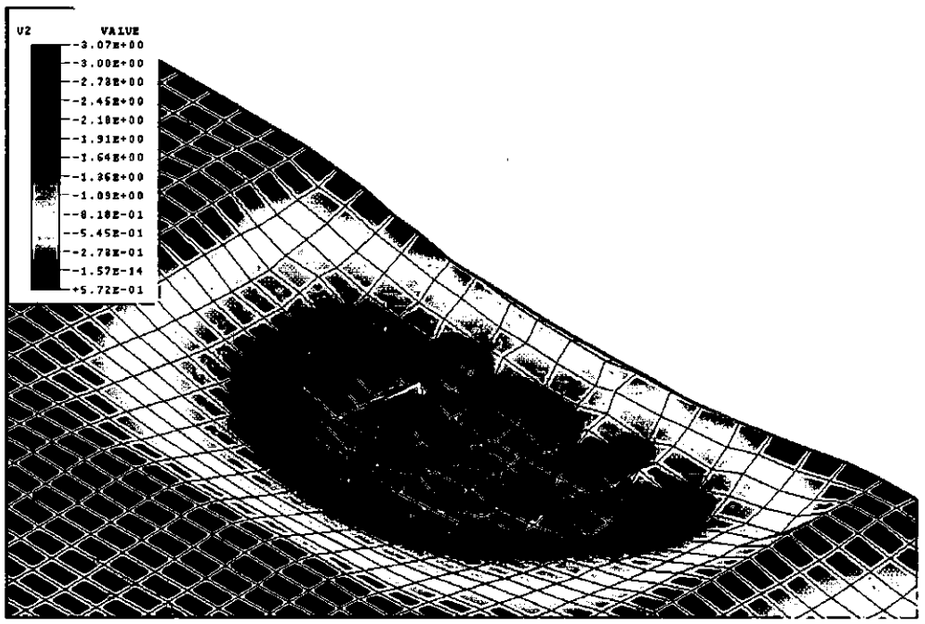

Figure 11
Dynamic Analysis - Load Case 1 - Close up of deck displacement

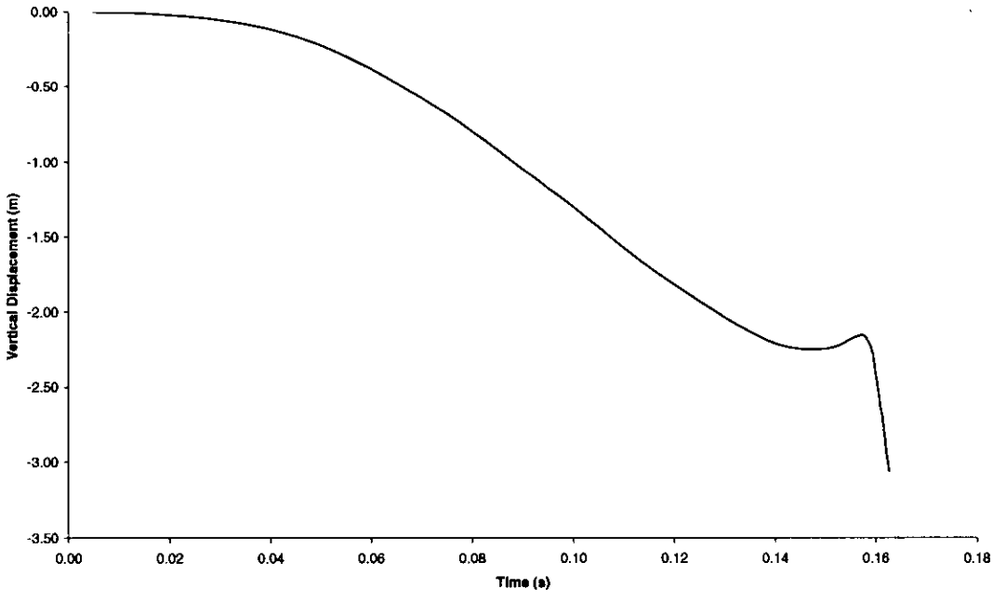

Figure 12
Displacement of centre of buckled deck panel.

Contents

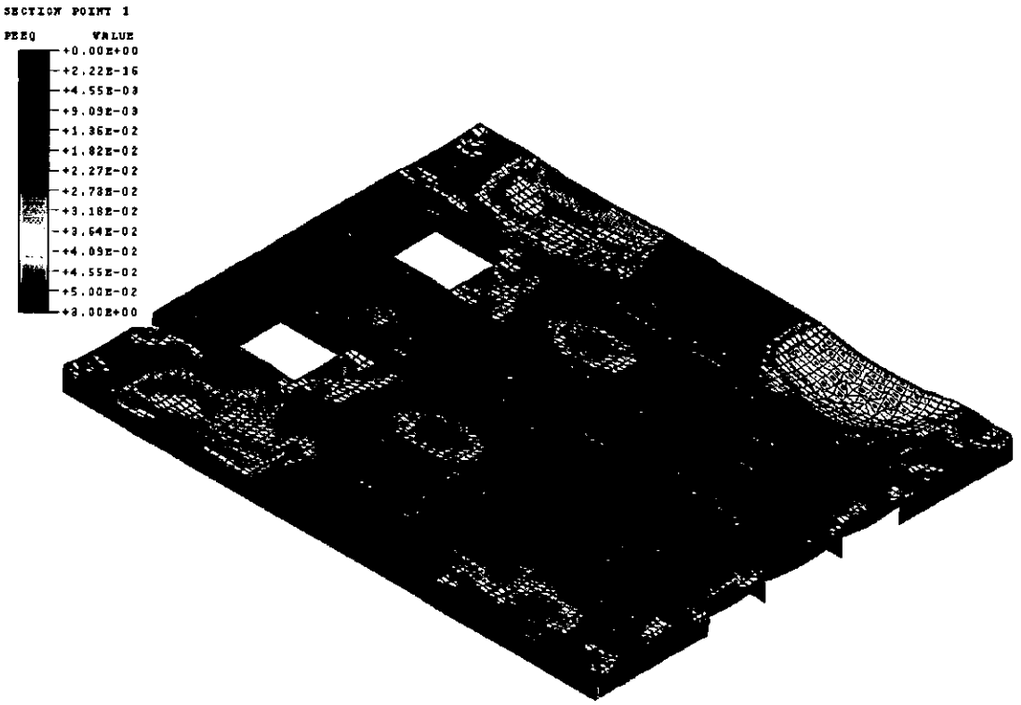

Figure 13
Contour plot of Plastic Equivalent Strain

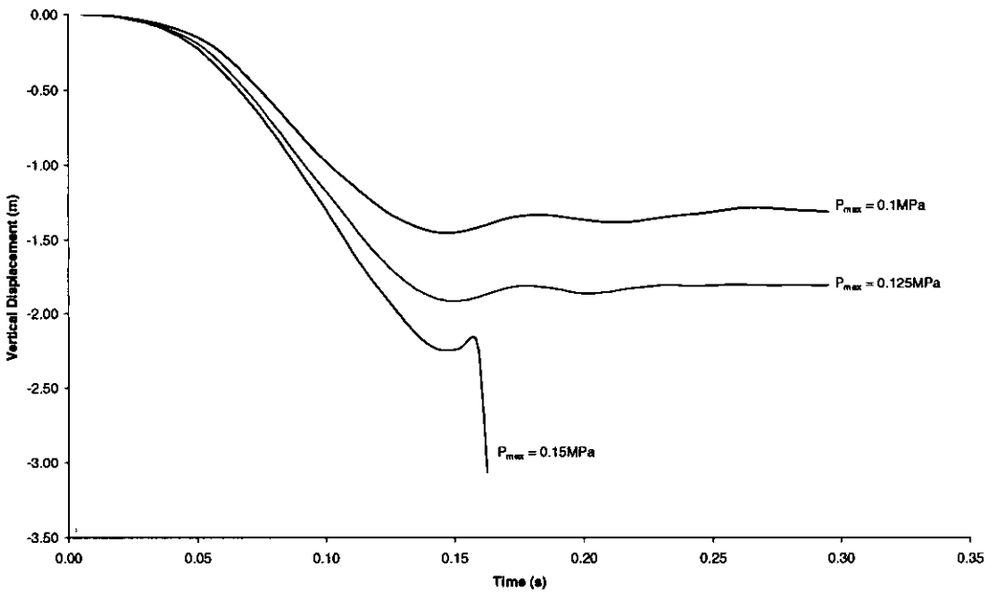

Figure 14
Displacement of centre of panel due to 0.1MPa, 0.125MPa and 0.15MPa

Contents

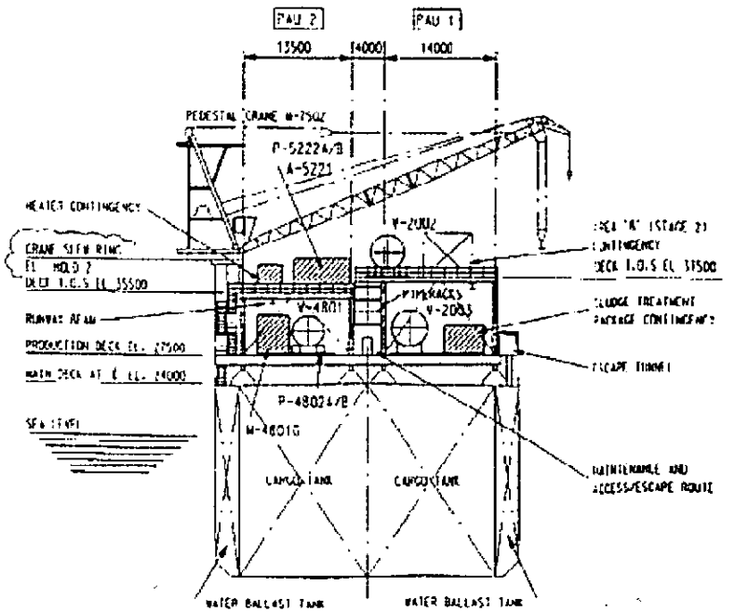

Figure 15
Vessel B - Frame details

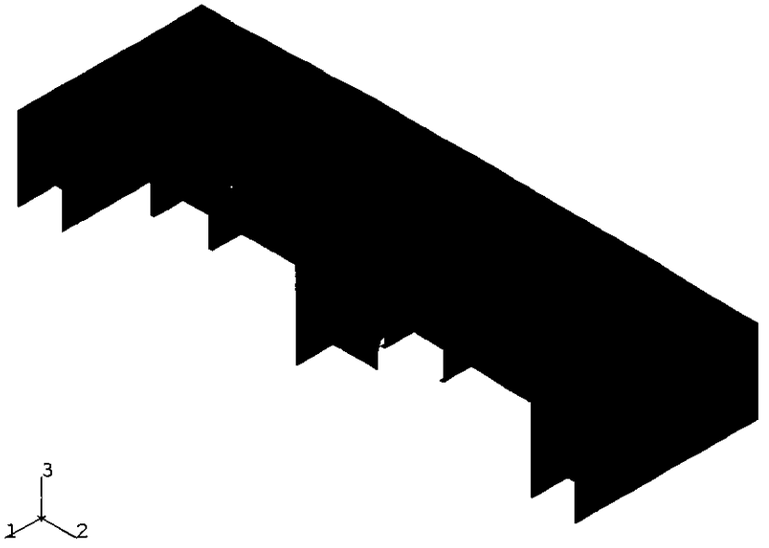

Figure 16
Vessel B - Finite element mesh

Contents

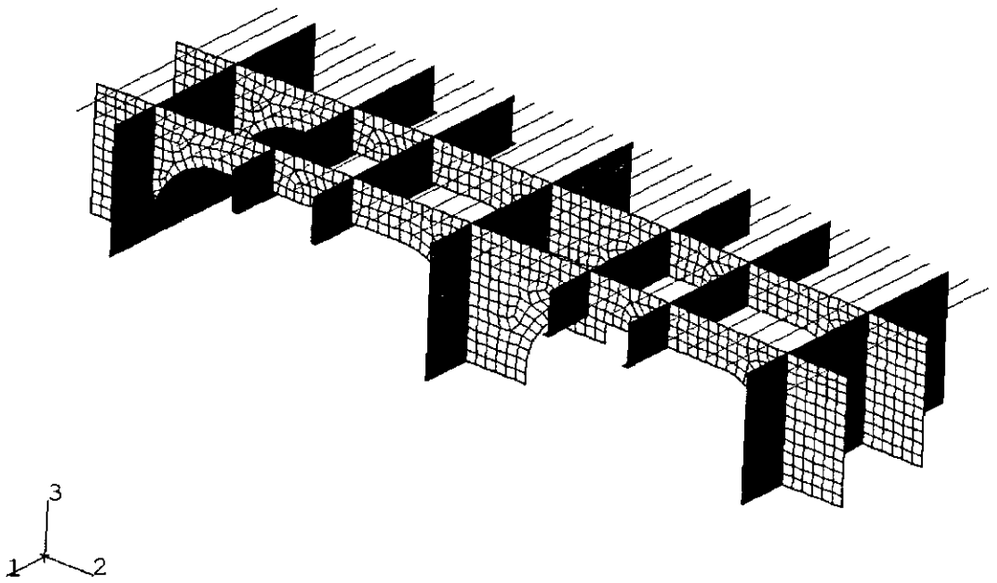

Figure 17
Vessel B - Supporting structure

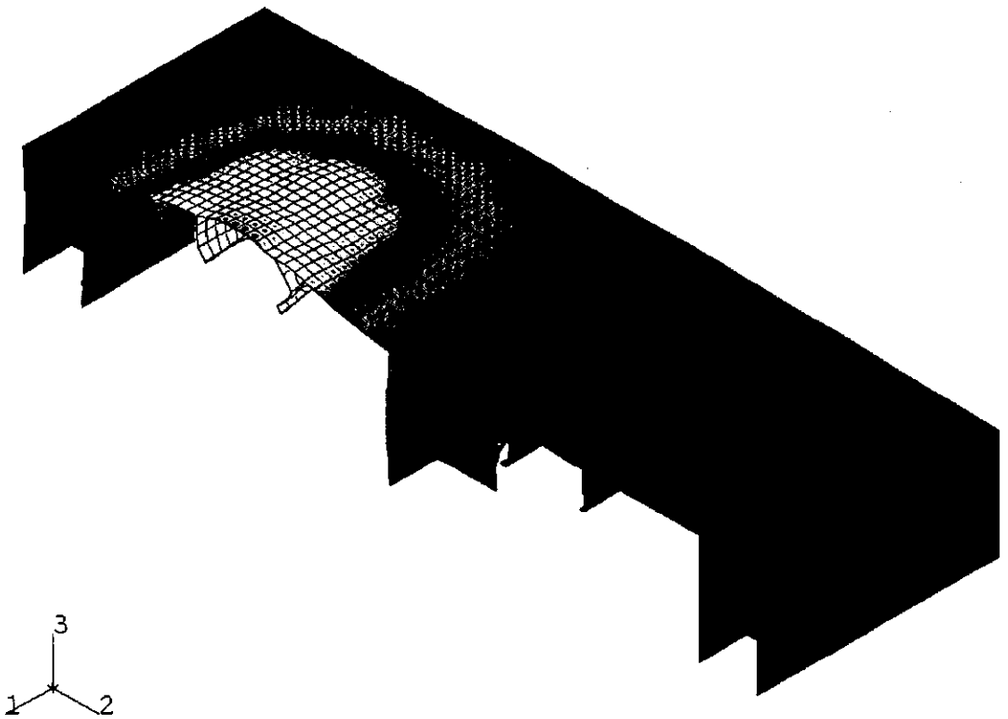

Figure 18
Vessel B - Starboard tank mode - Eigenmode 67 - 27.5Hz

Contents

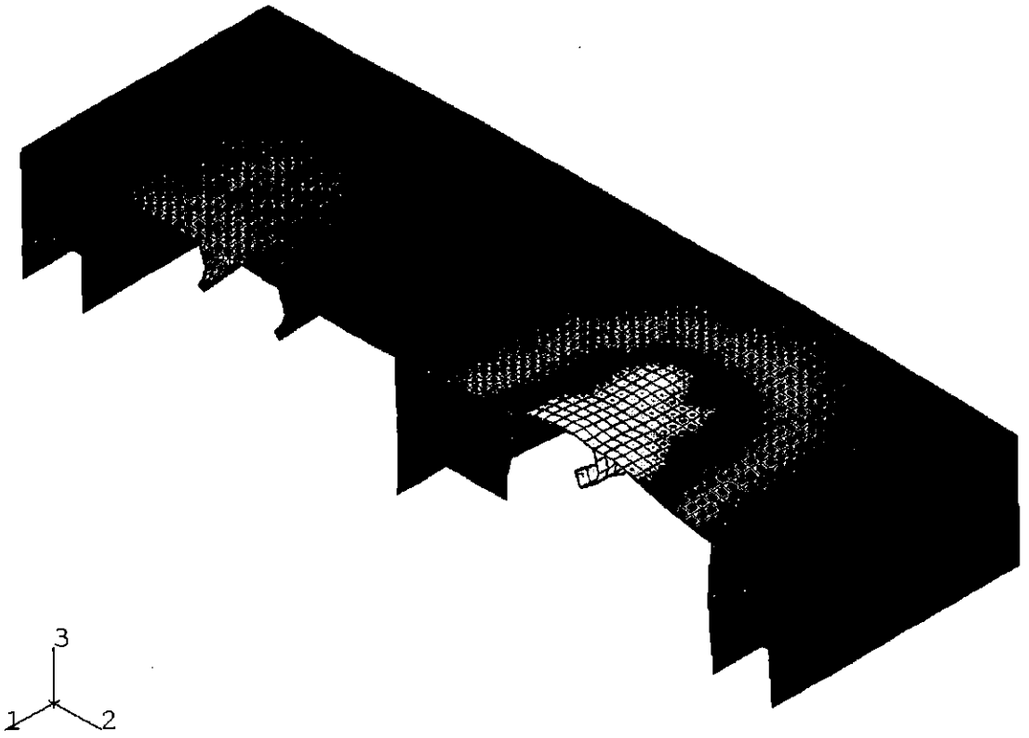

Figure 19
Vessel B - Port tank mode - Eigenmode 86 - 34.1Hz

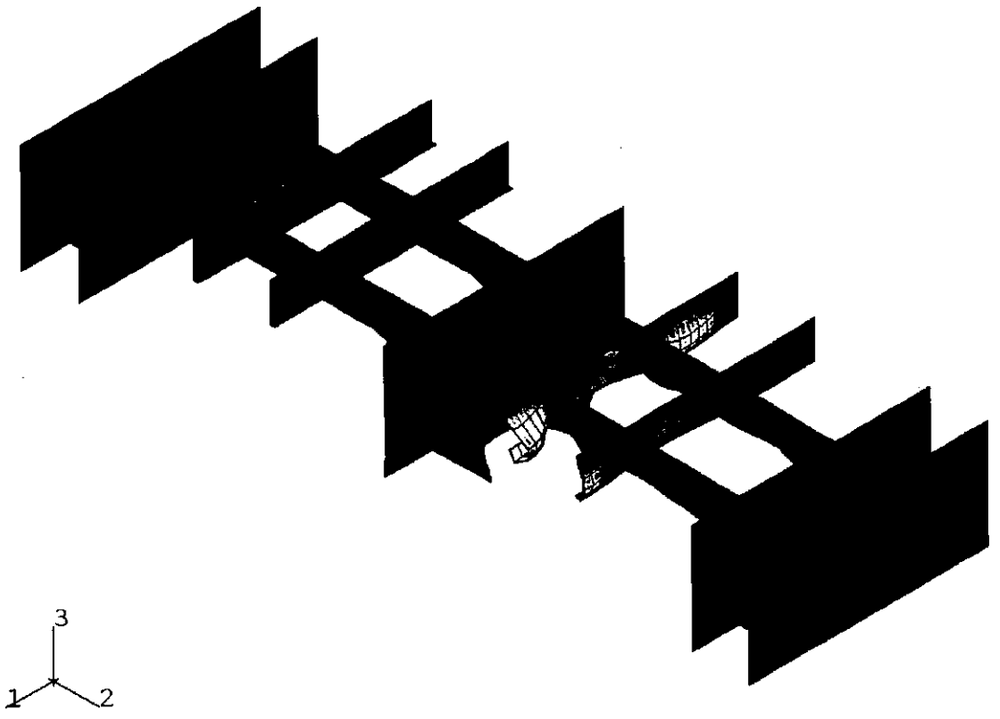

Figure 20
Vessel B - Eigenmode 30 - 17.2Hz

Contents

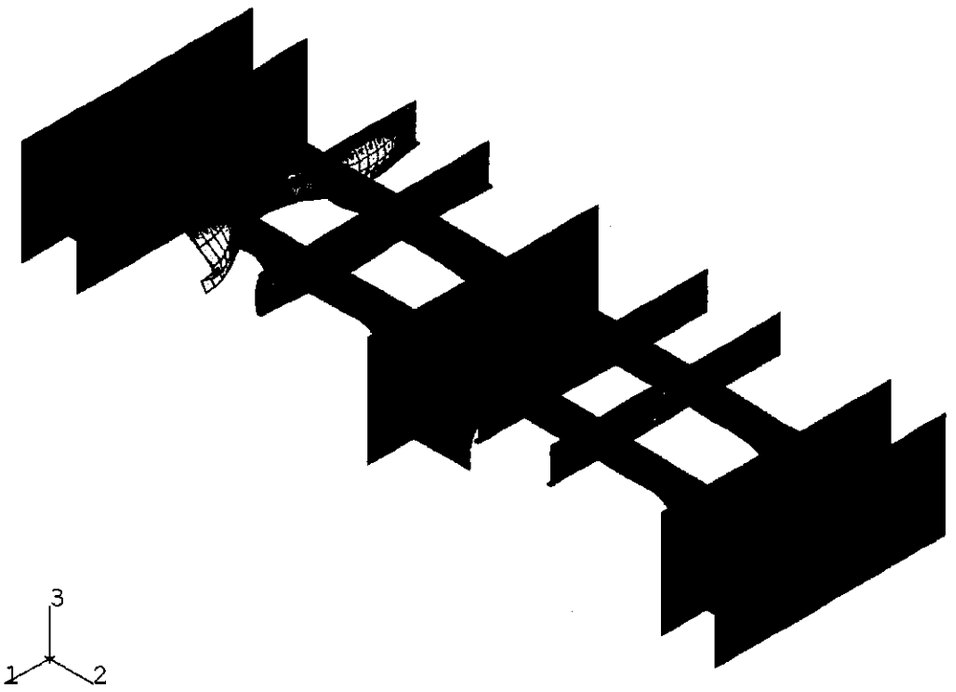

Figure 21
Vessel B - Eigenmode 32 - 17.5Hz

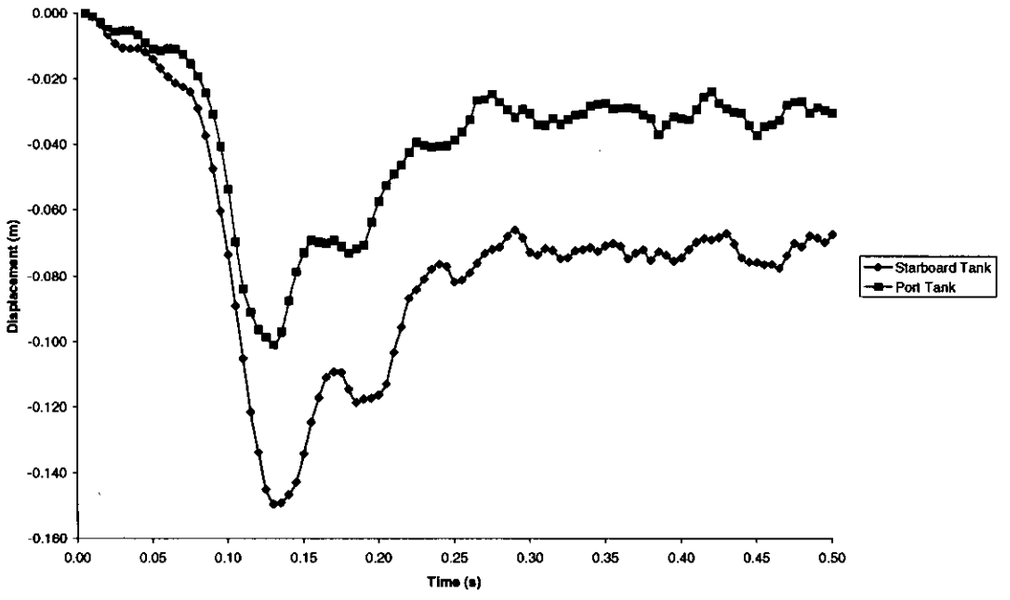

Figure 22
Displacement of Port & Starboard Tanks - Load Case 1

Contents

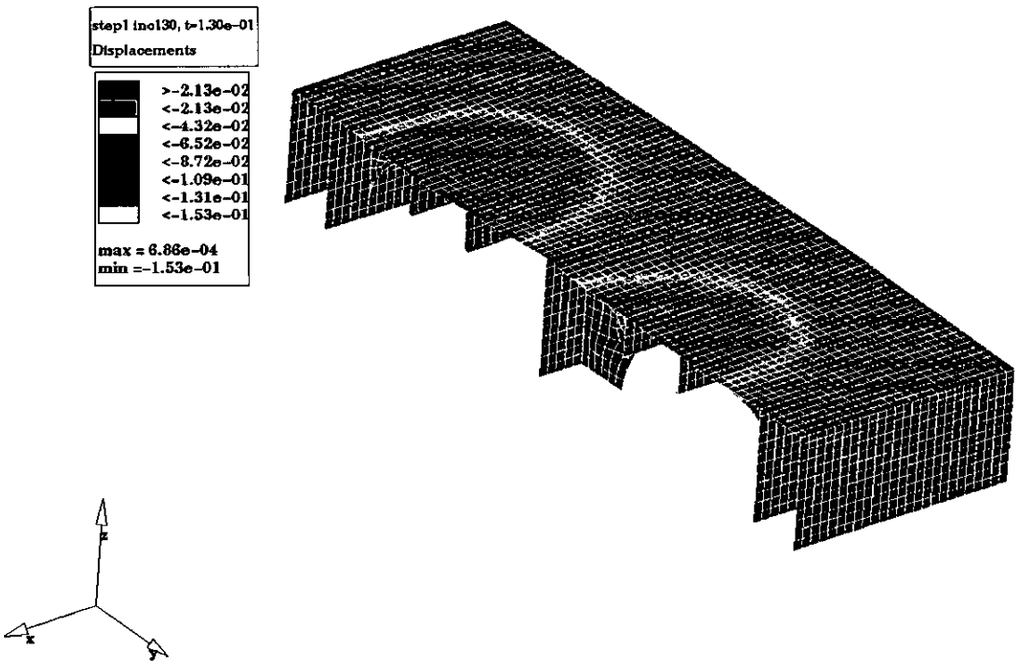

Figure 23
Displacement contour plot - Load Case 1, 130ms

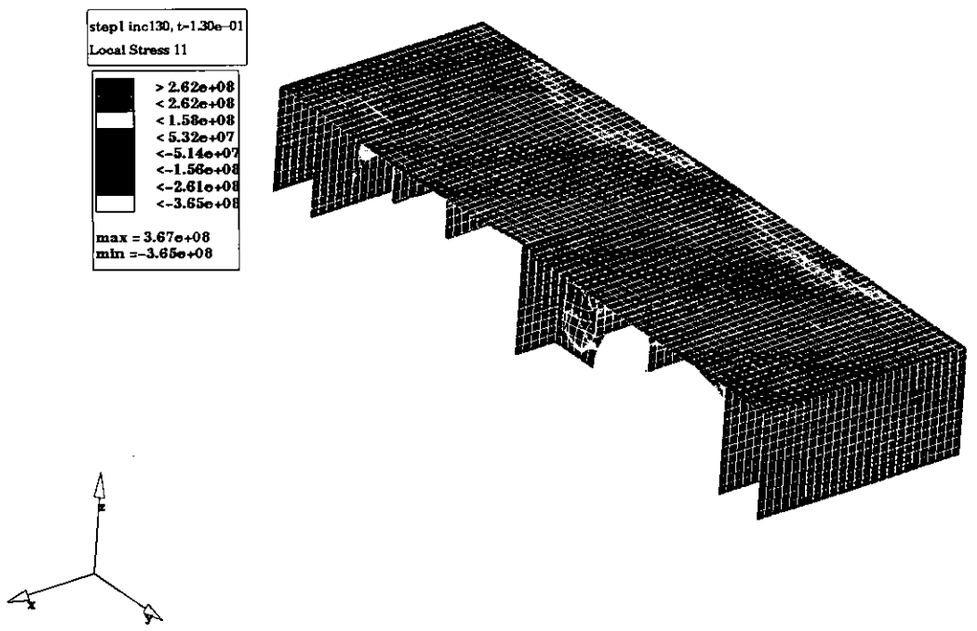

Figure 24
Stress (Fore/Aft) contour plot - Load Case 1, 130ms

Contents

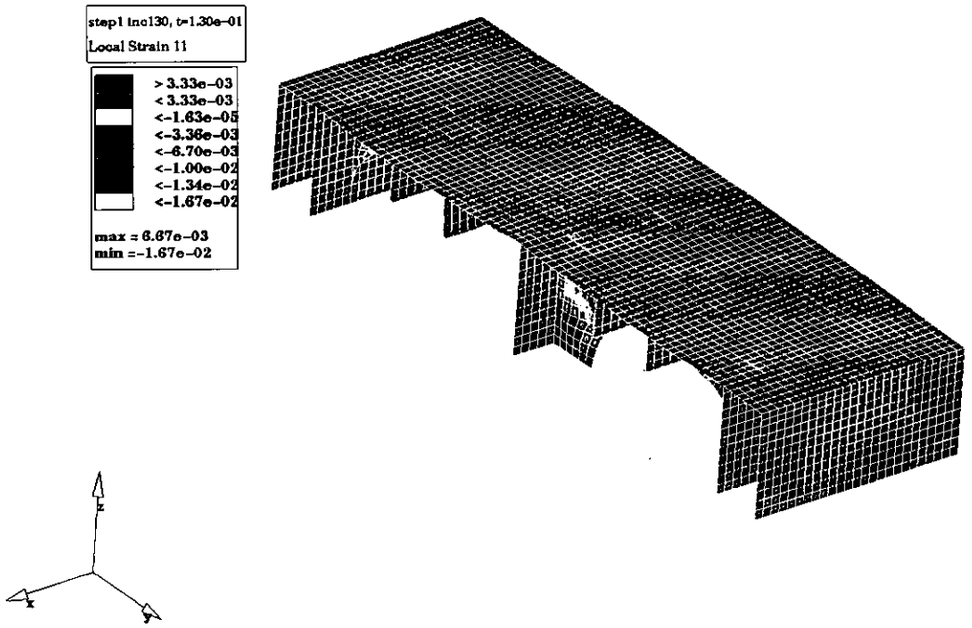

Figure 25
Strain (Fore/Aft) contour plot - Load Case 1, 130ms

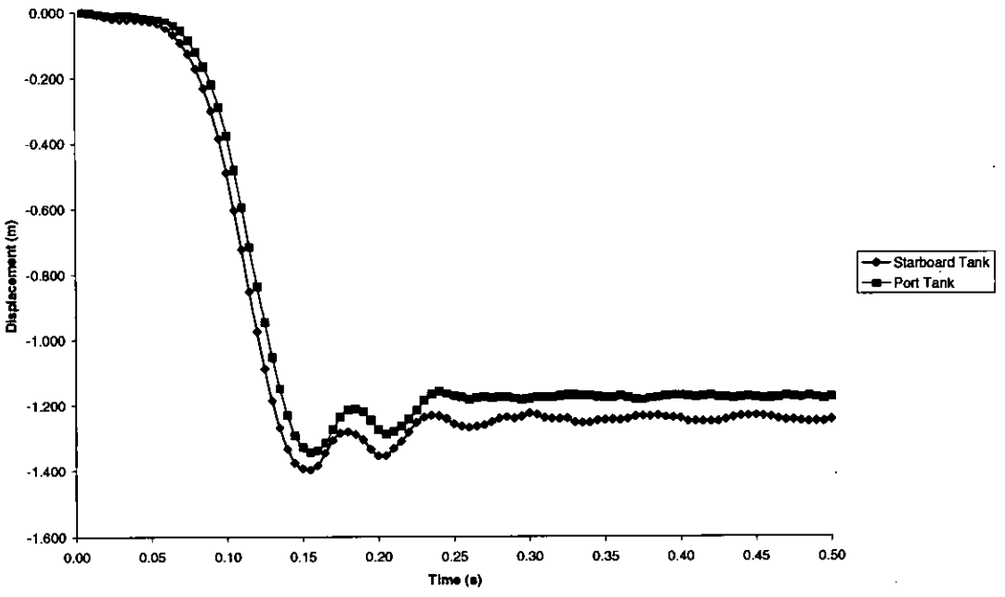

Figure 26
Displacement of Port & Starboard Tanks - Load Case 2

Contents

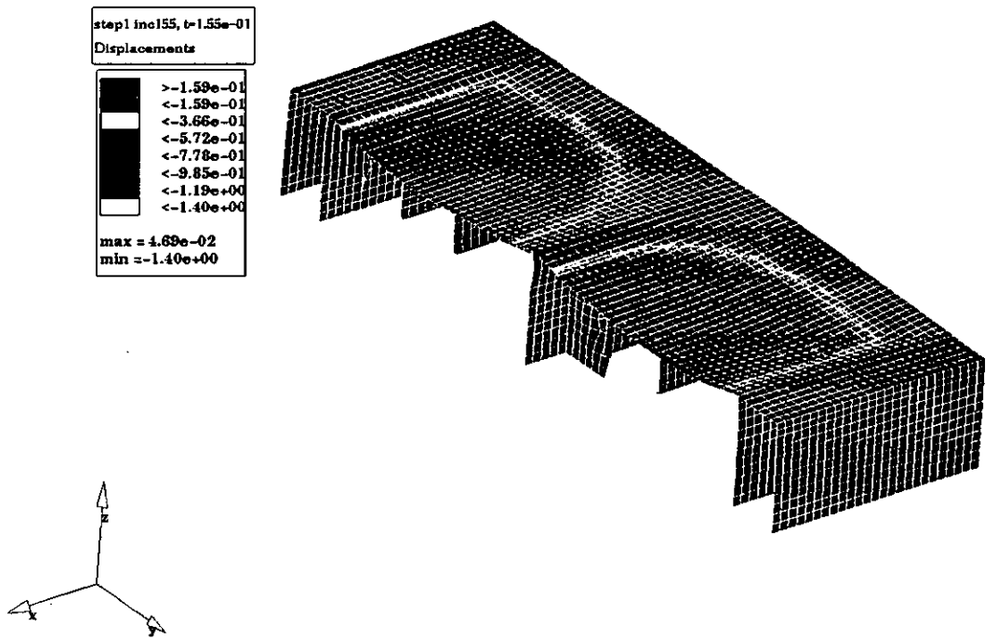

Figure 27
Displacement contour plot - Load Case 2, 155ms

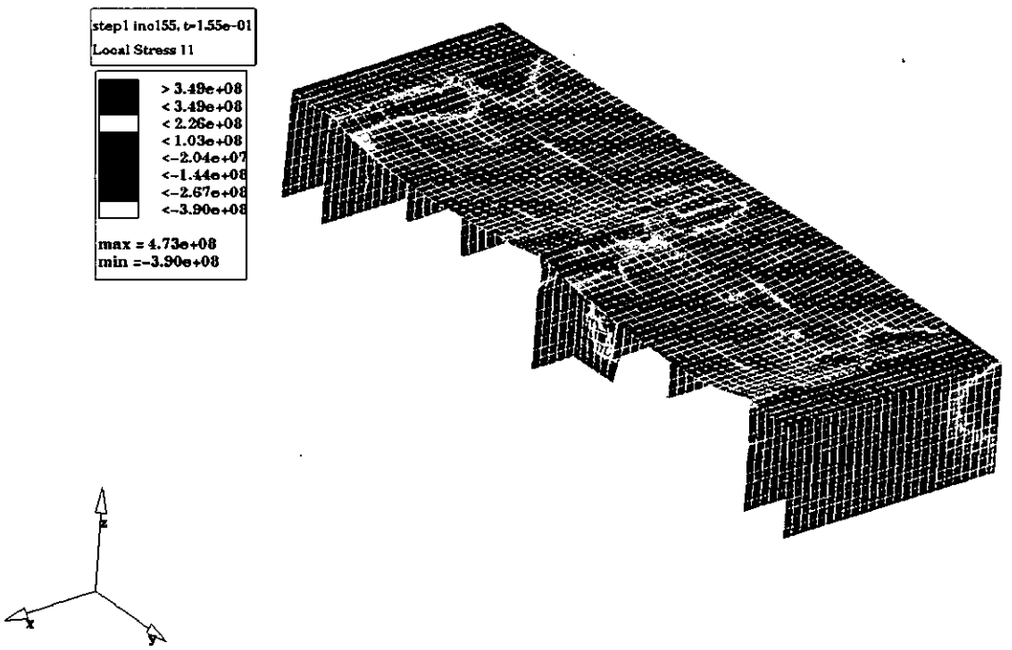

Figure 28
Stress (Fore/Aft) contour plot - Load Case 2, 155ms

Contents

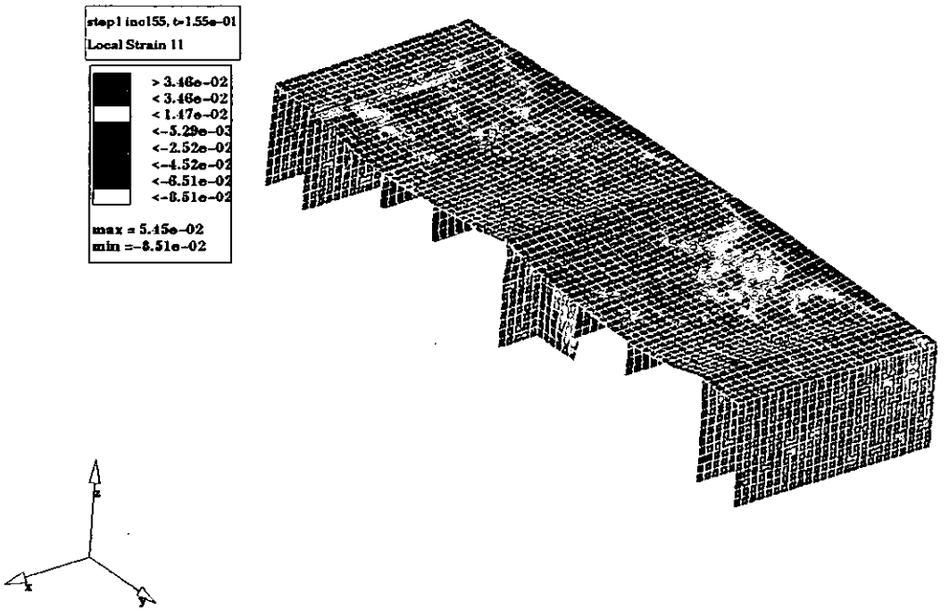

Figure 29
Strain (Fore/Aft) contour plot - Load Case 2, 155ms

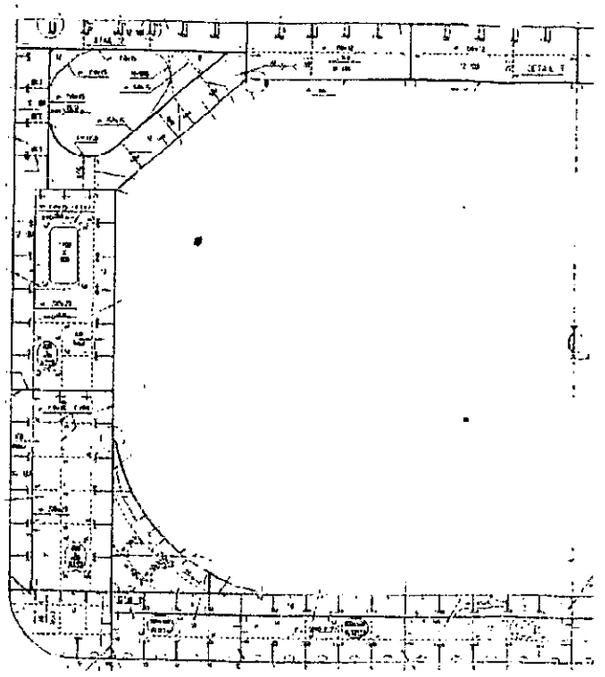

Figure 30
Vessel C - Typical Frame details

Contents

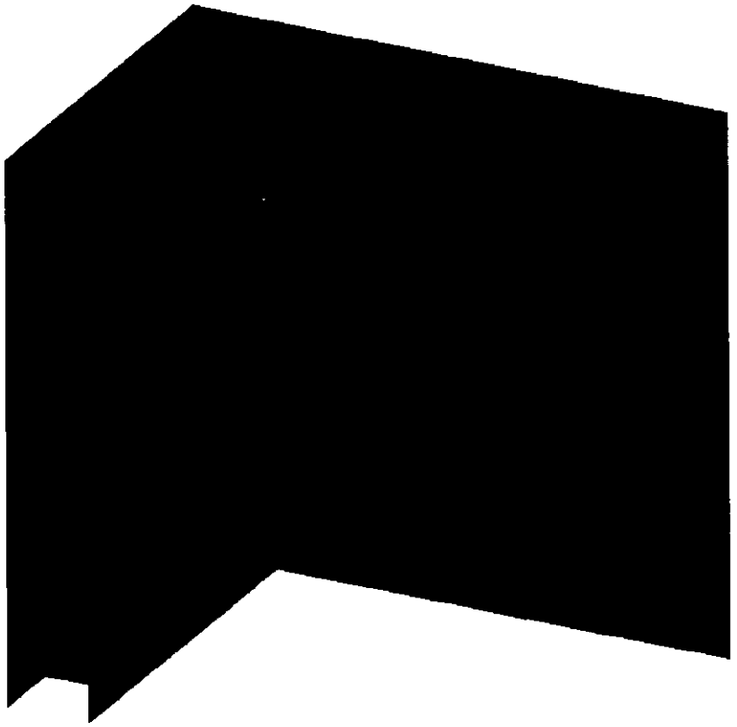

Figure 31
Vessel C - FE model

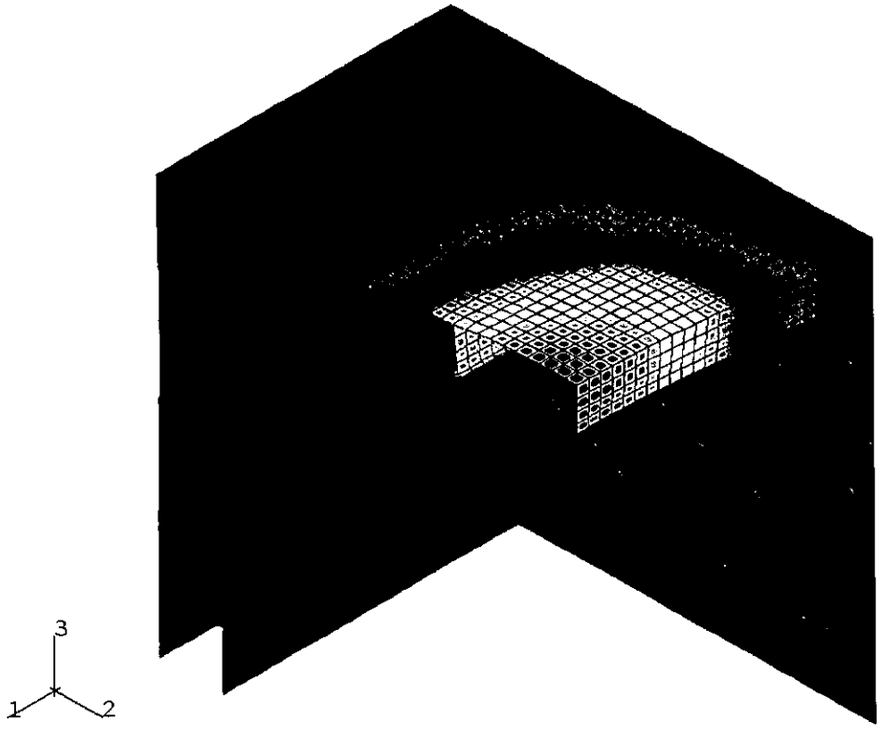

Figure 32
Vessel C - Eigenmode 13 - 15.0Hz

Contents

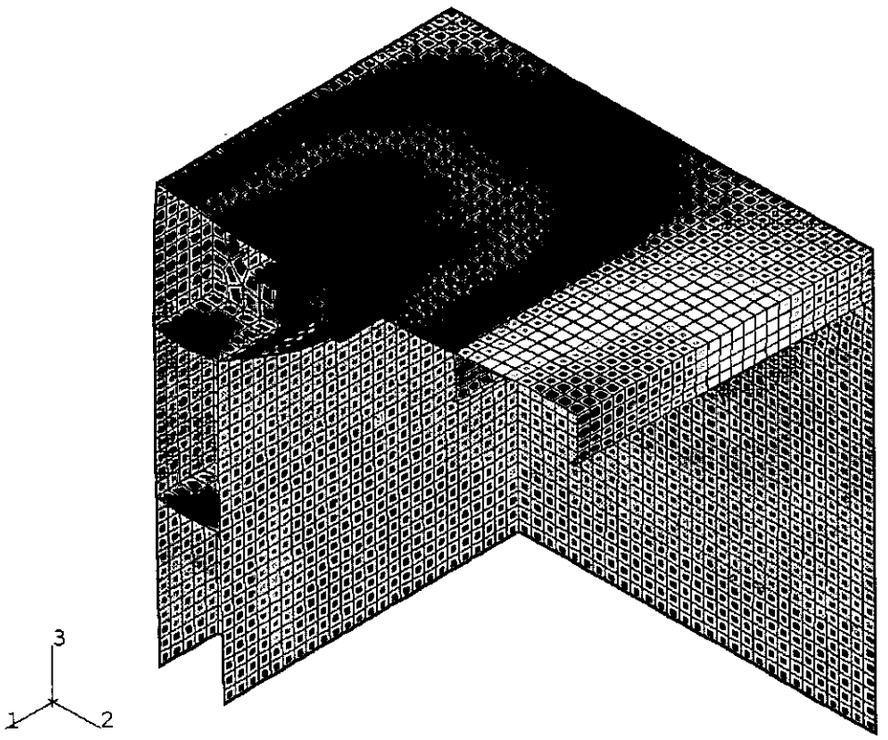

Figure 33
Vessel C - Eigenmode 36 - 25.1Hz

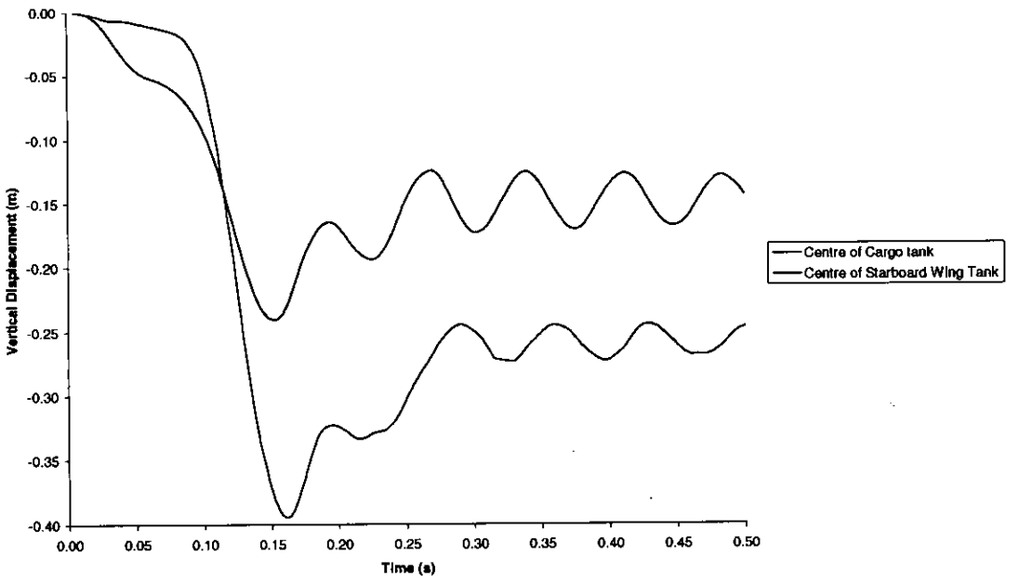

Figure 34
Displacement of centre tank and starboard wing tank - Load Case 1

Contents

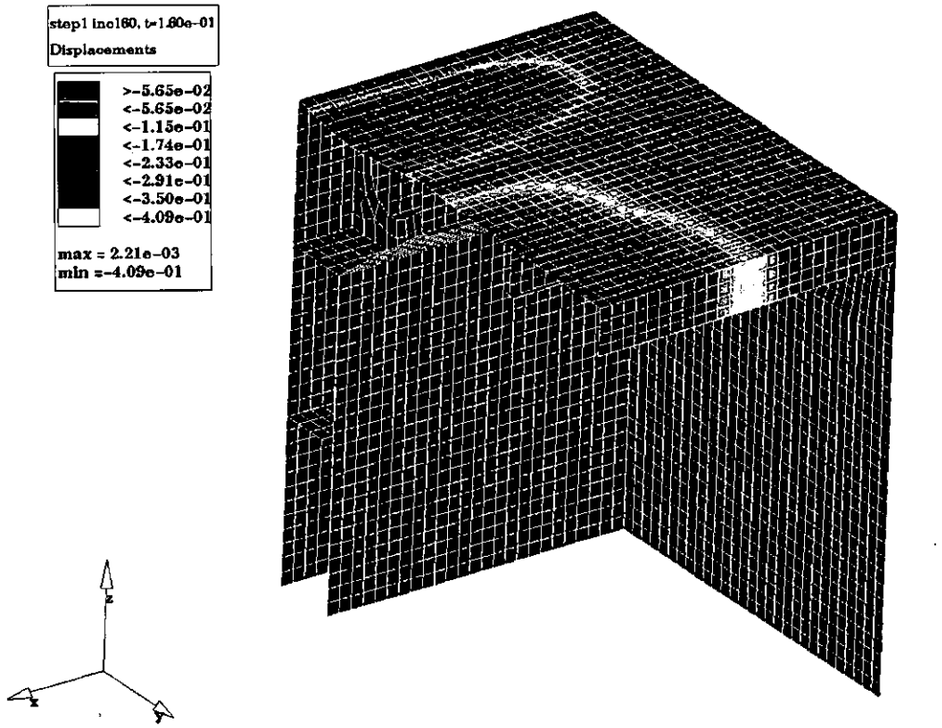

Figure 35
Displacement contour plot - Load Case 1, 160ms

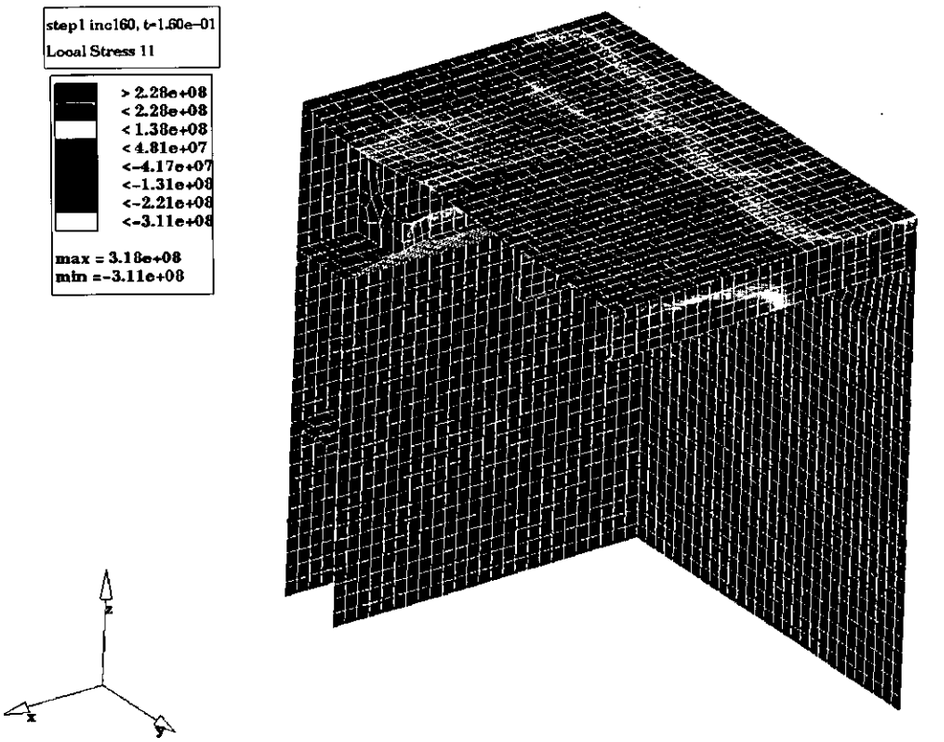

Figure 36
Stress (Fore/Aft) contour plot - Load Case 1, 160ms

Contents

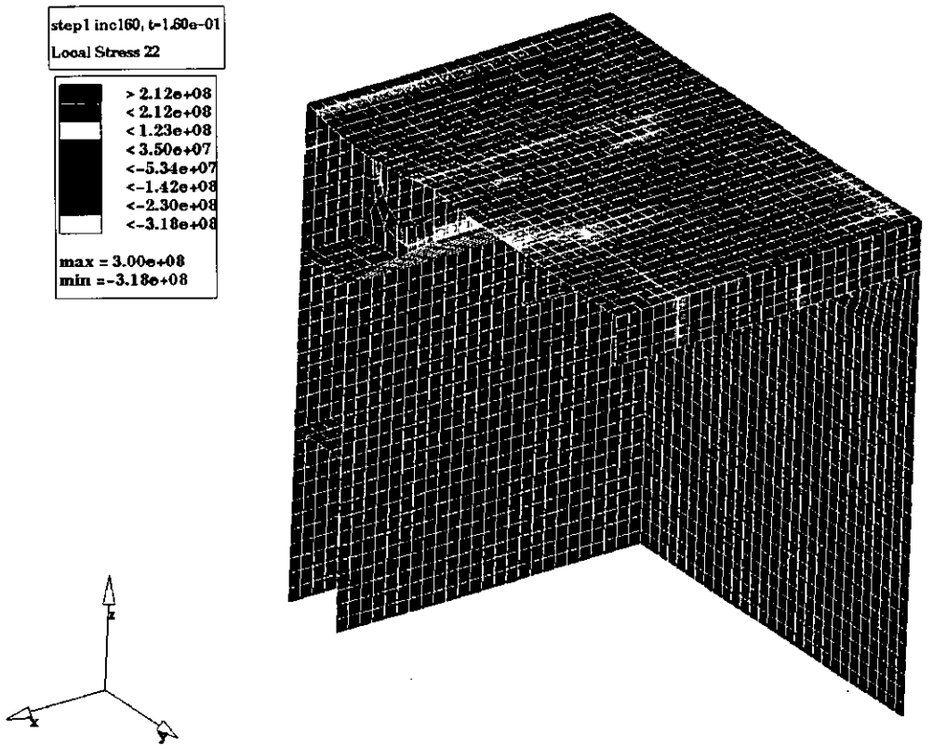

Figure 37
Stress (Port/Stbd) contour plot - Load Case 1, 160ms

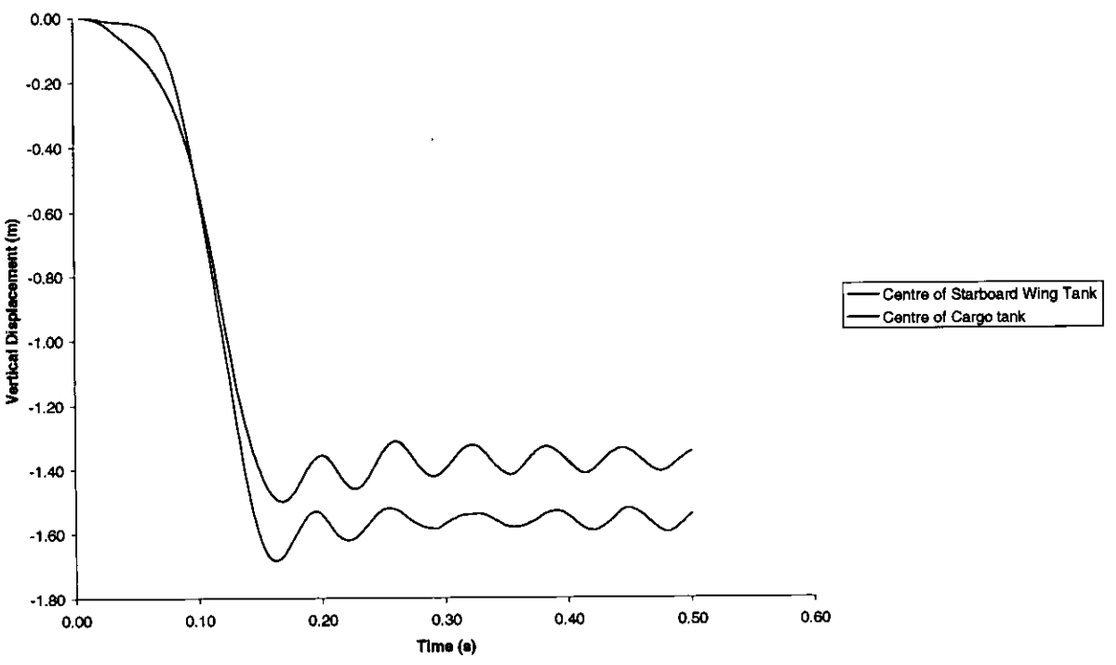

Figure 38
Displacement of centre tank and starboard wing tank - Load Case 2

Contents

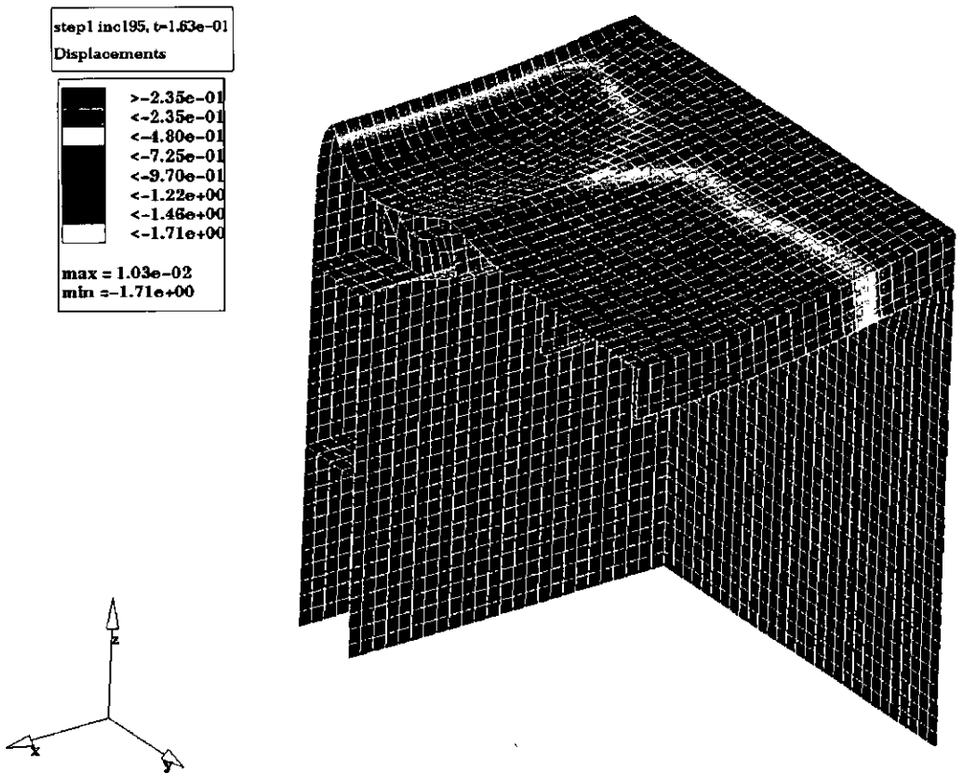

Figure 39
Displacement contour plot - Load Case 2, 163ms

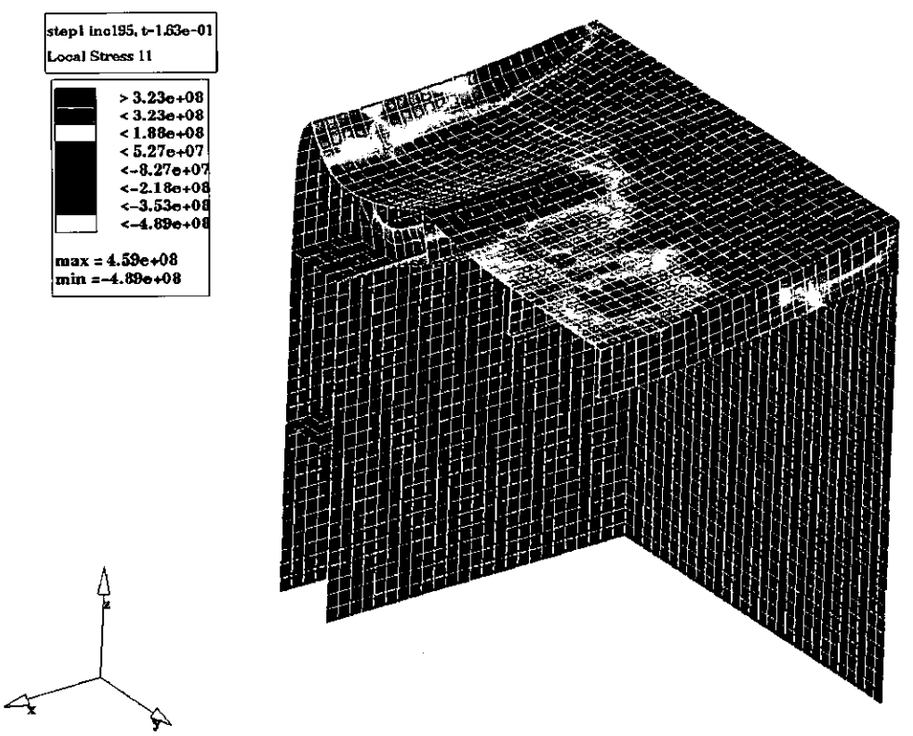

Figure 40
Stress (Fore/Aft) contour plot - Load Case 2, 163ms

Contents

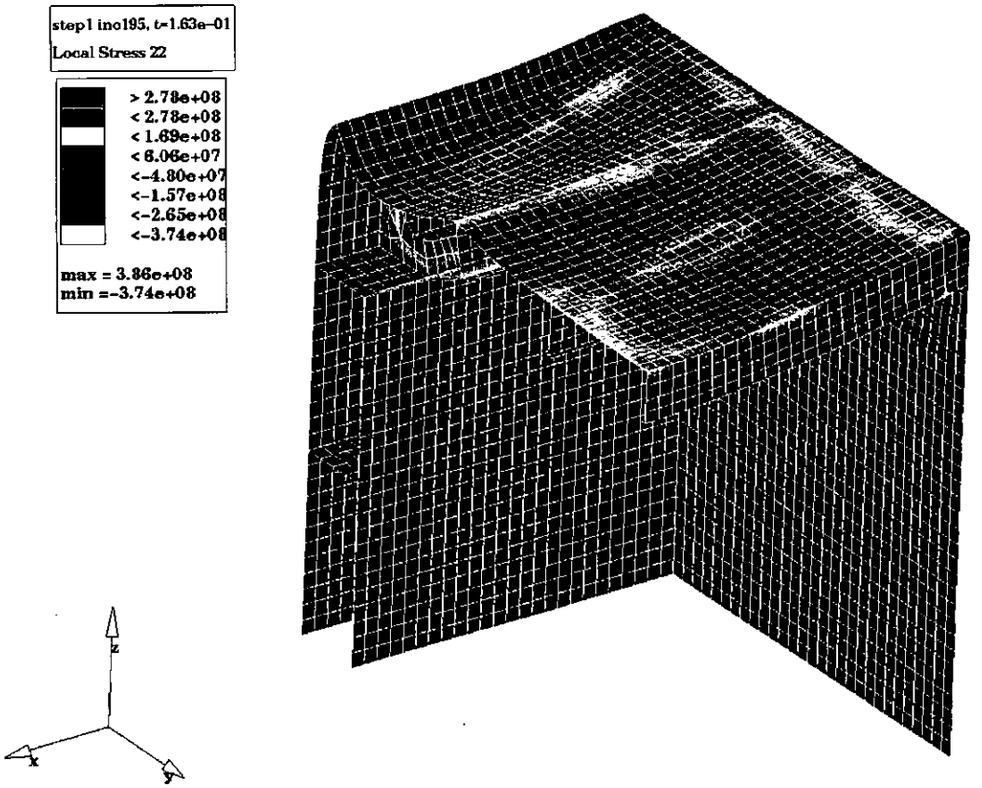

Figure 41
Stress (Port/Stbd) contour plot - Load Case 2, 163ms

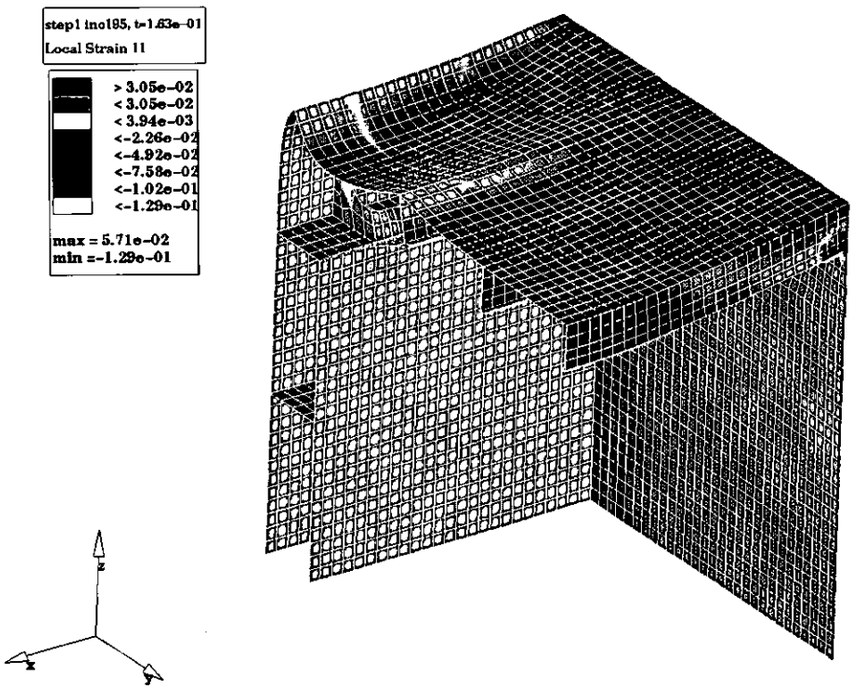

Figure 42
Strain (Fore/Aft) contour plot - Load Case 2, 163ms

Contents

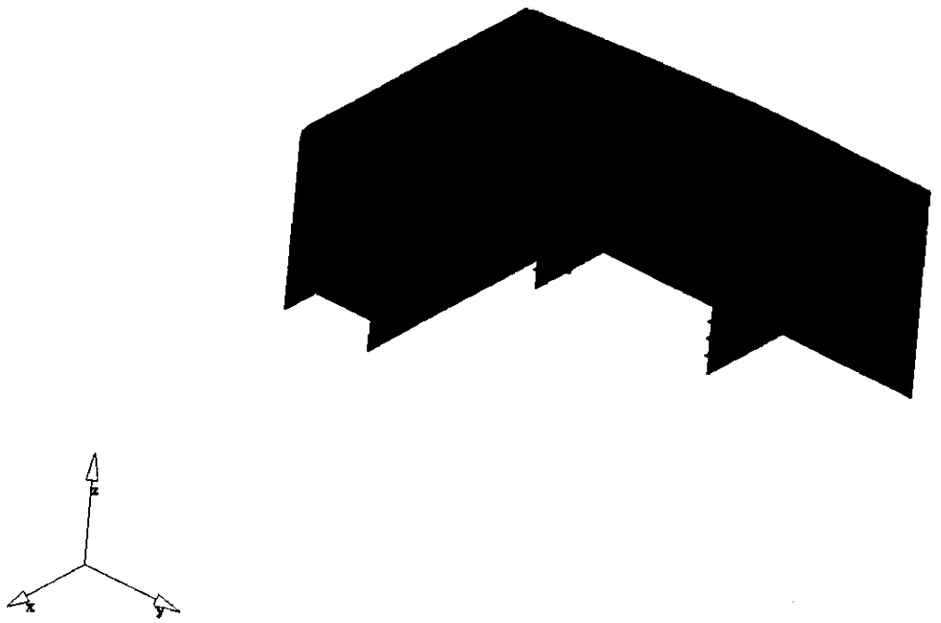

Figure 43
Vessel D - FE model

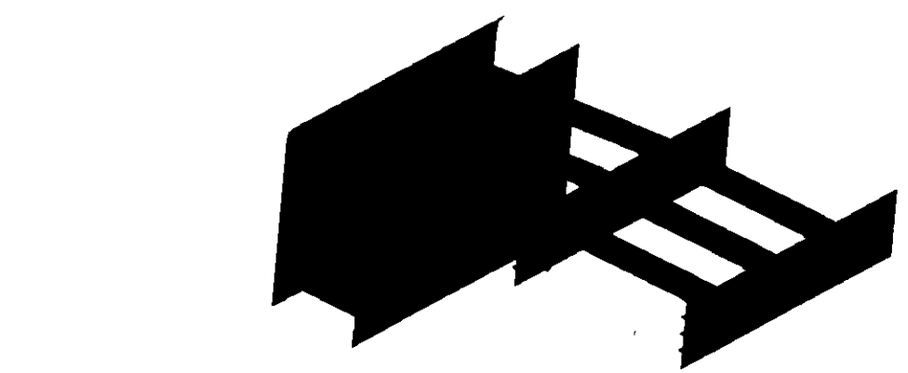

Figure 44
Vessel D - Internal FE model detail

Contents

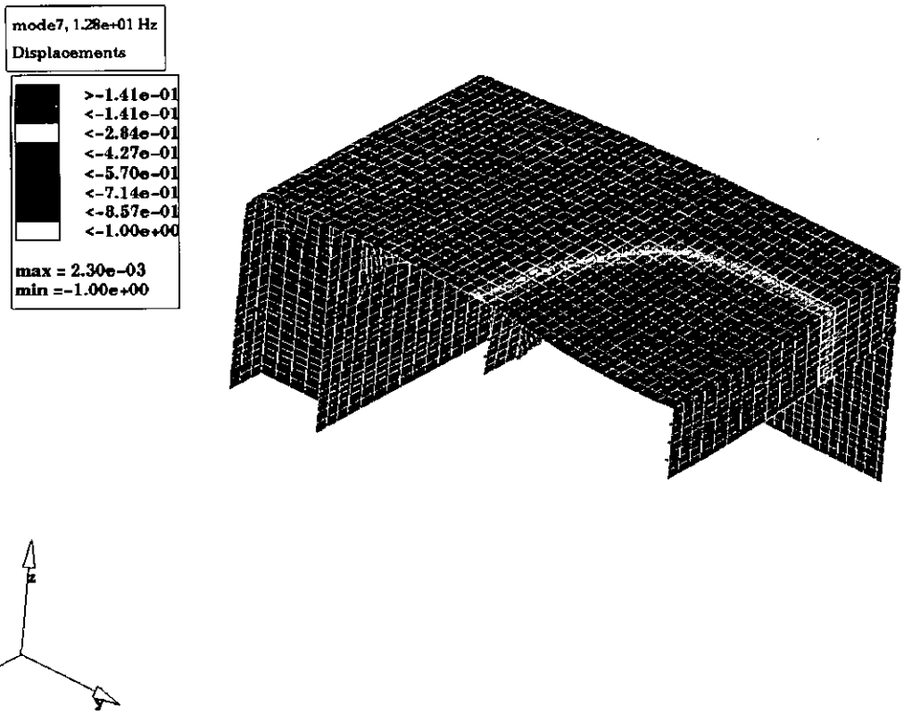

Figure 45
Vessel D - Eigenmode 7 - 12.8Hz

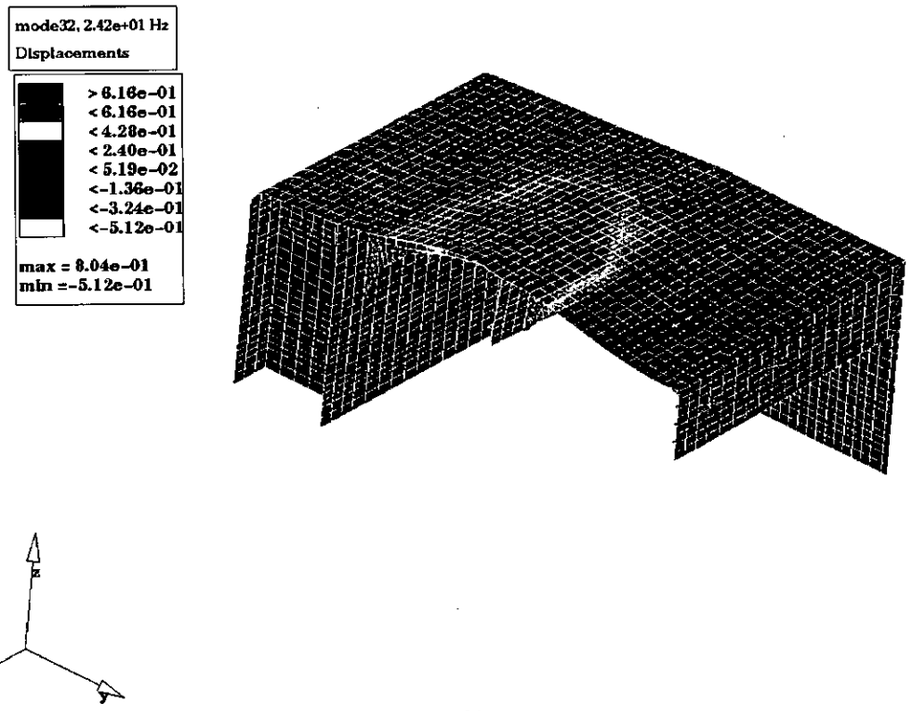

Figure 46
Vessel D - Eigenmode 36 - 24.2Hz

Contents

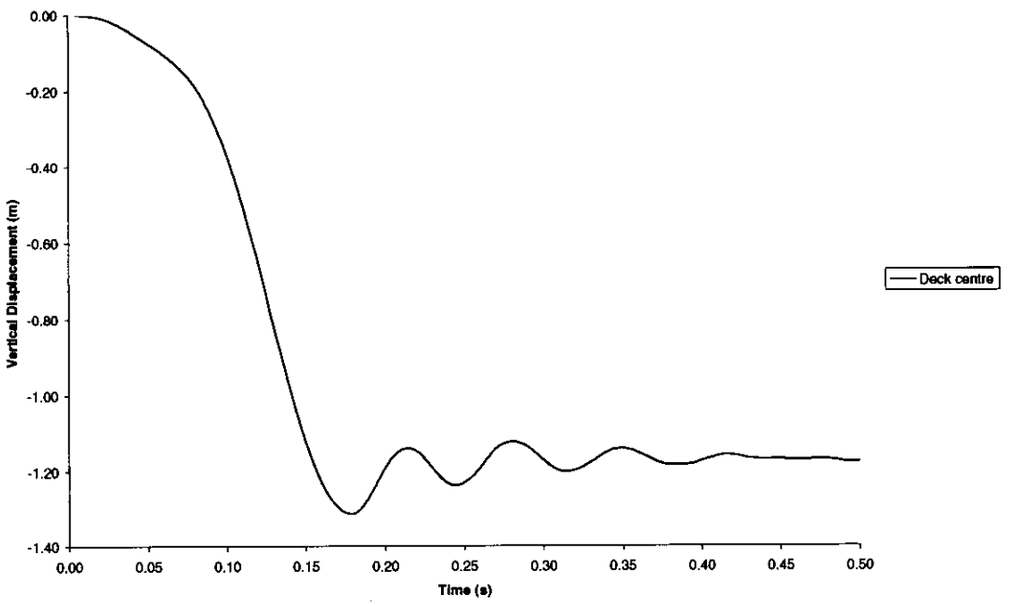

Figure 47
Displacement of cargo tank centre - Load Case 1

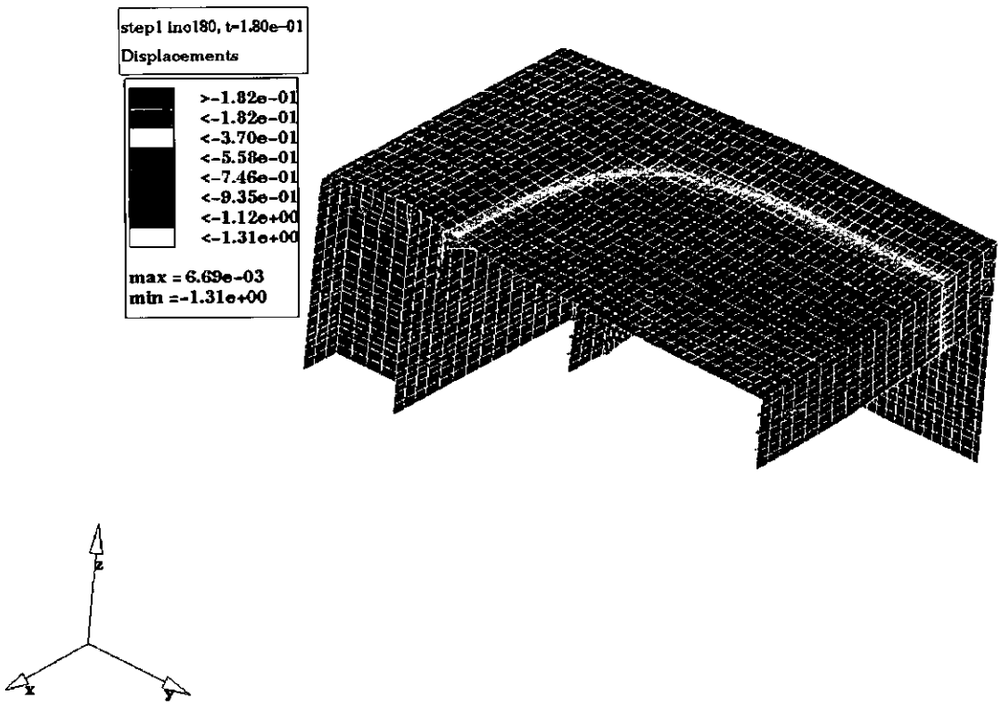

Figure 48
Displacement contour plot - Load Case 1, 180ms

Contents

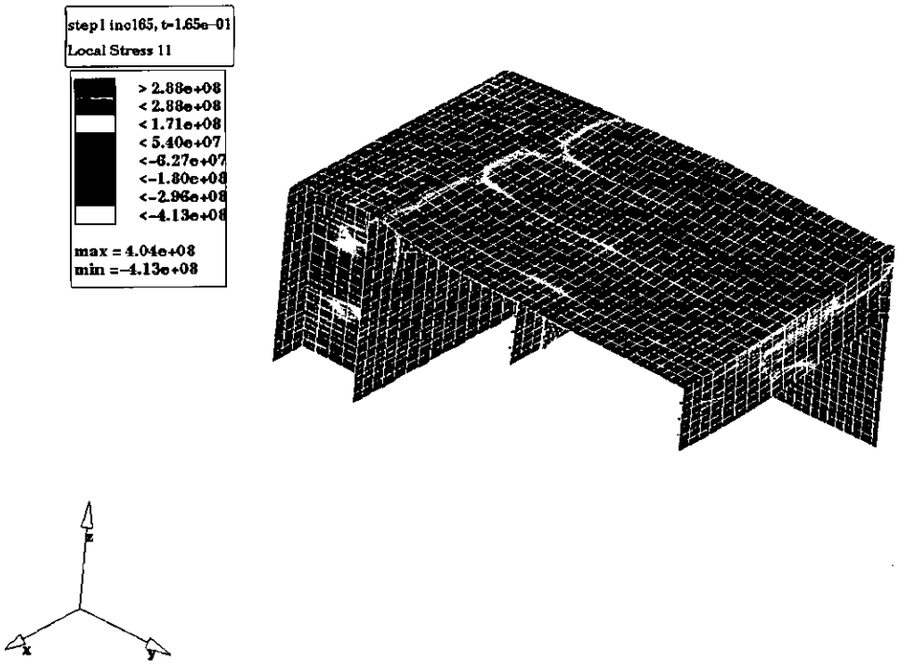

Figure 49
Stress (Fore/Aft) contour plot - Load Case 1, 180ms

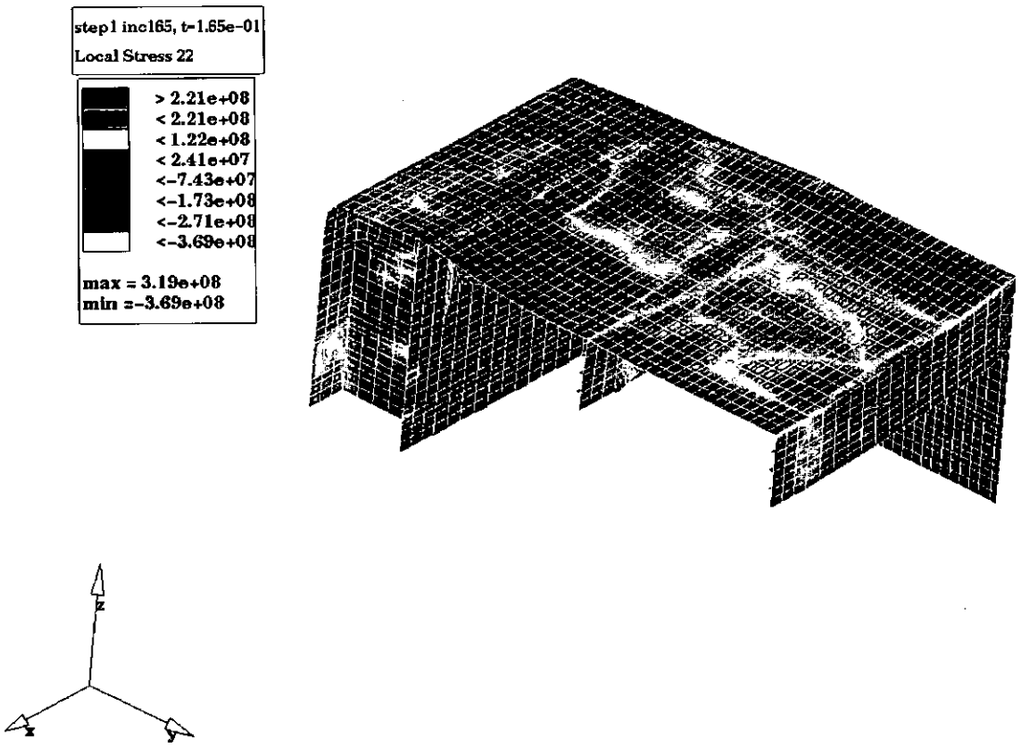

Figure 50
Stress (Port/Sfbd) contour plot - Load Case 1, 180ms

Contents

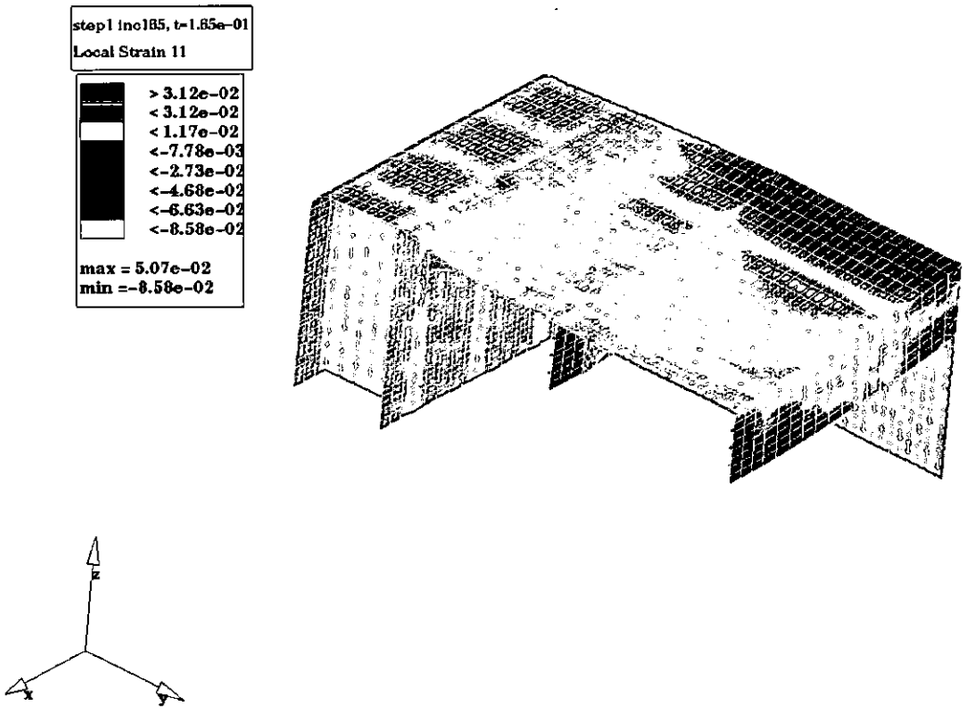

Figure 51
Strain (Fore/Aft) contour plot - Load Case 1, 180ms

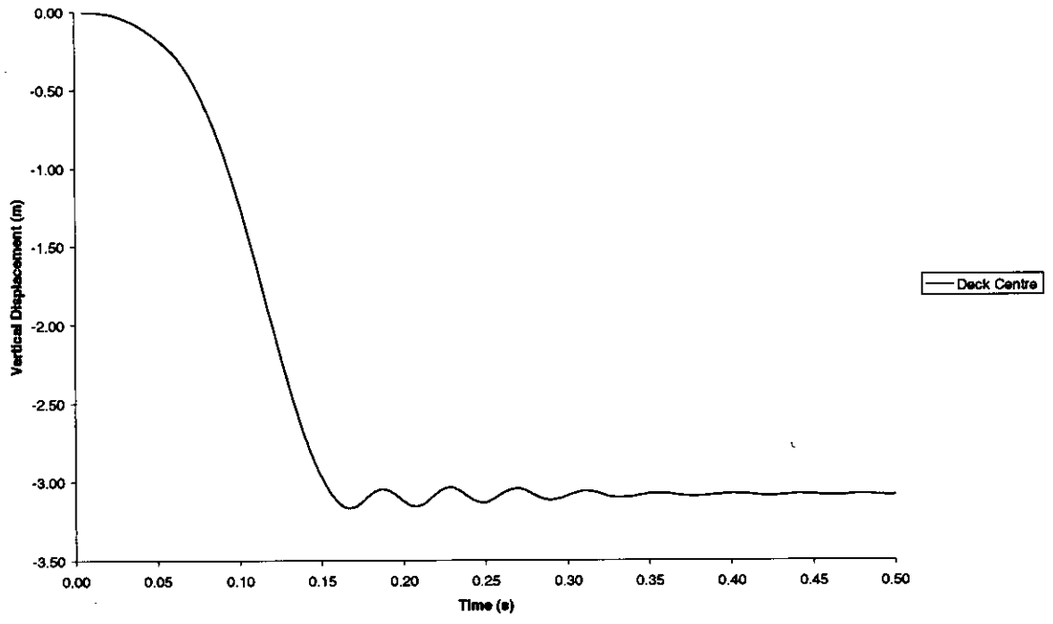

Figure 52
Displacement of centre of tank - Load Case 2

Contents

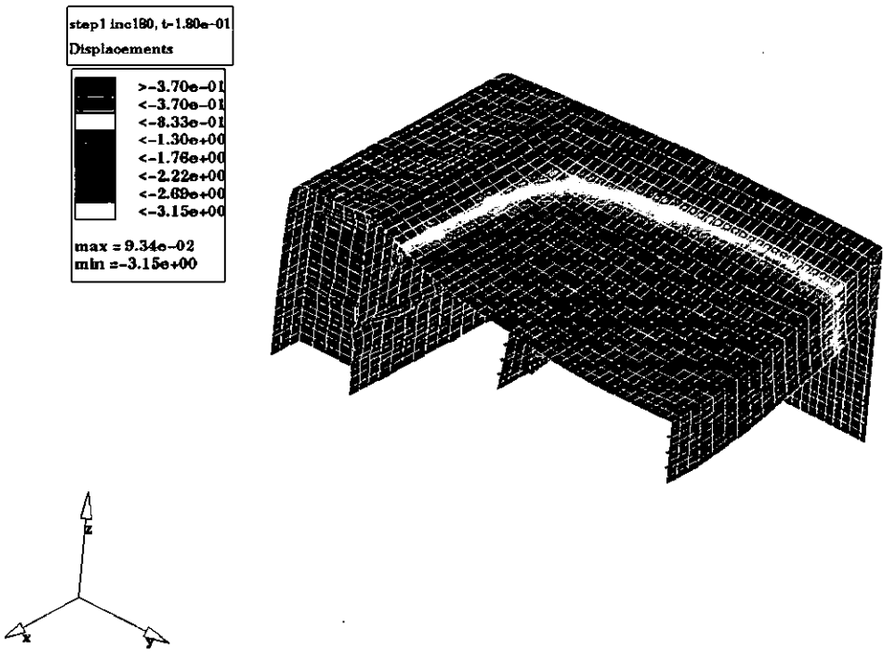

Figure 53
Displacement contour plot - Load Case 2, 165ms

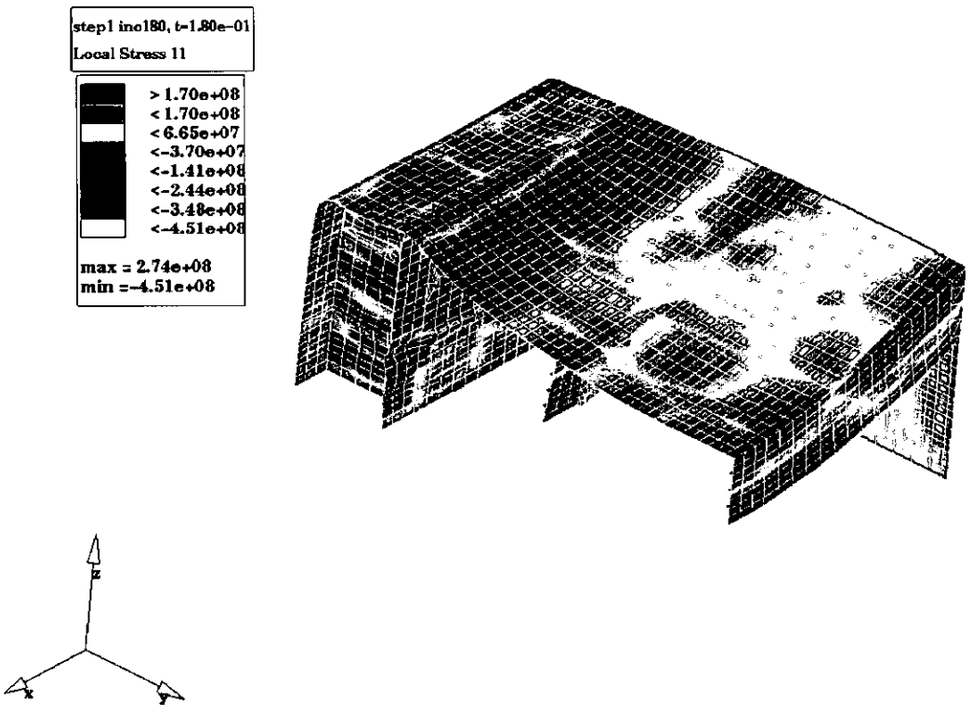

Figure 54
Stress (Fore/Aft) contour plot - Load Case 2, 165ms

Contents

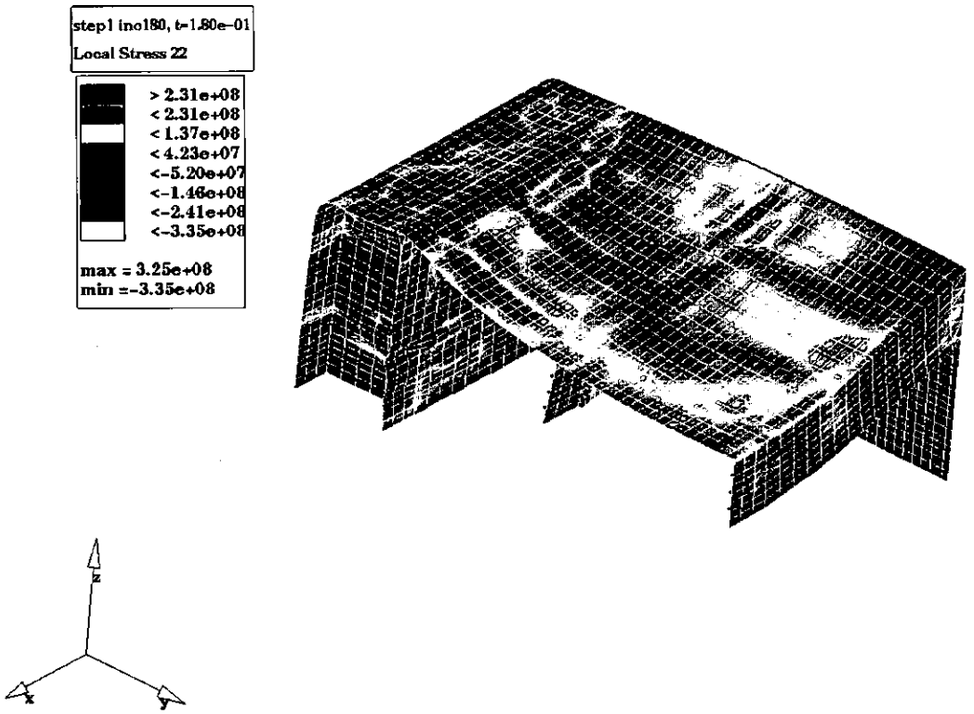

Figure 55
Stress (Port/Stbd) contour plot - Load Case 2, 165ms

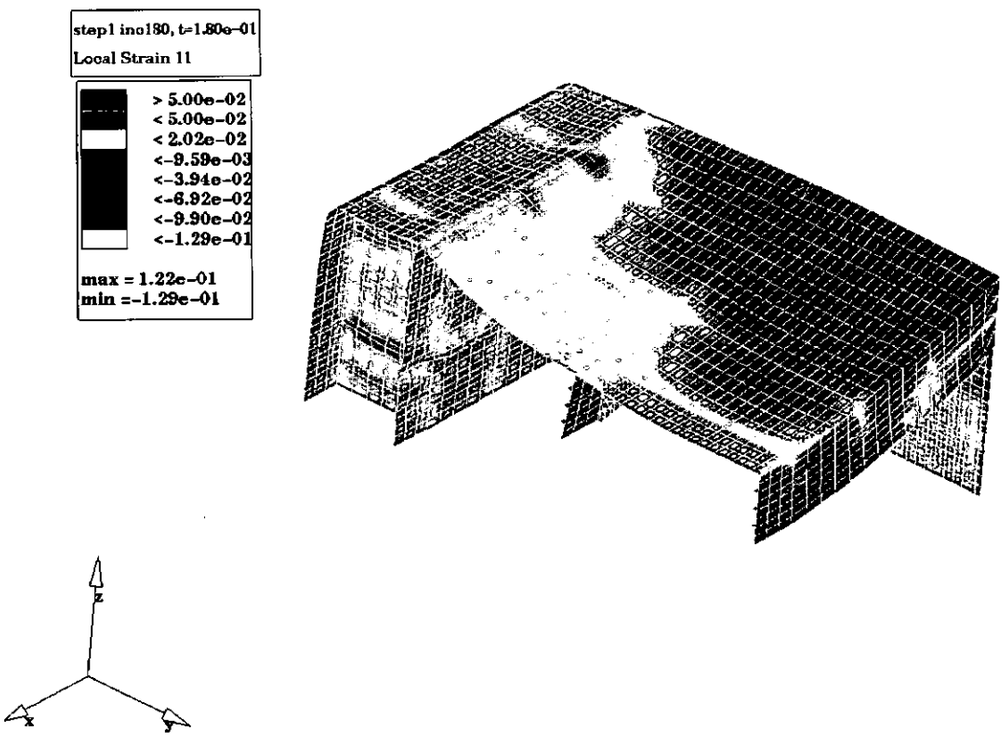

Figure 56
Strain (Fore/Aft) contour plot - Load Case 2, 165ms

Contents

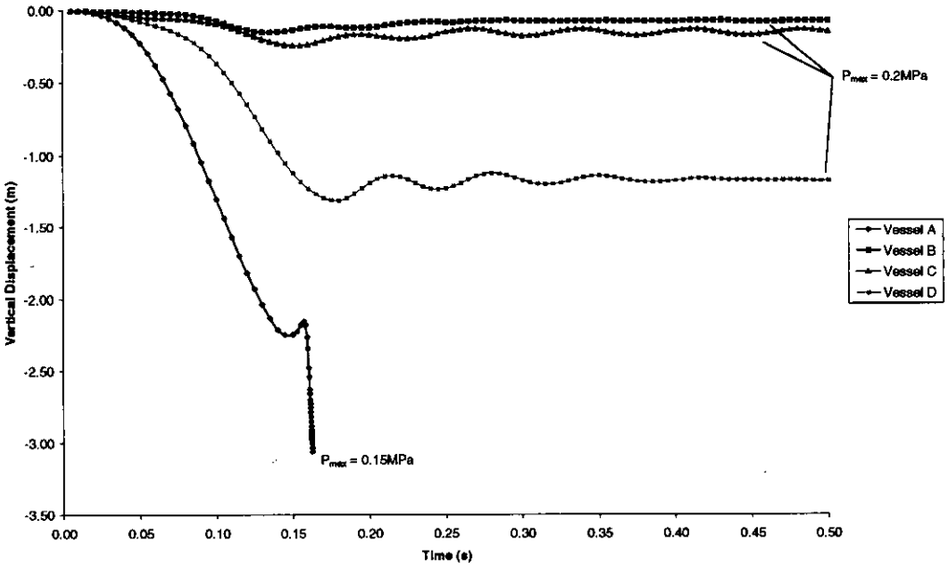

Figure 57
Comparison of responses - Load Case 1 (2 bar)

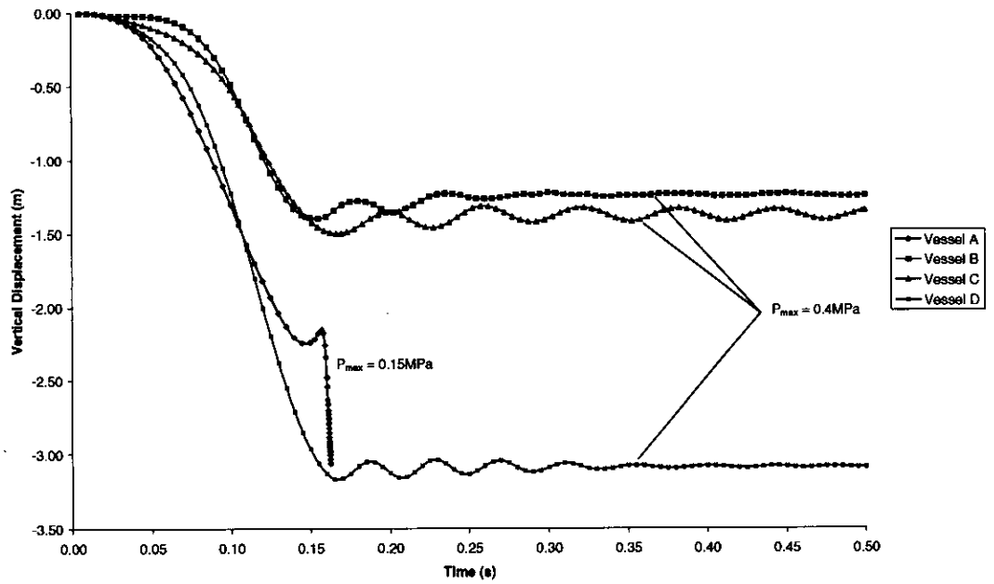

Figure 58
Comparison of response - Load Case 2 (4 bar)

Contents